CRCLEME

Cooperative Research Centre for
Landscape Environments
and Mineral Exploration

CSIRO

OPEN FILE
REPORT
SERIES

REGIONAL GEOCHEMICAL DISPERSION IN MATERIALS ASSOCIATED WITH ACID SULFATE SOILS IN RELATION TO BASE-METAL MINERALISATION OF THE KANMANTOO GROUP, MT TORRENS-STRATHALBYN REGION, EASTERN MT LOFTY RANGES, SOUTH AUSTRALIA.

M.S. Skwarnecki and R.W. Fitzpatrick

CRC LEME OPEN FILE REPORT 205

December 2008

CRCLEME

(CRC LEME Restricted Report 185R, 2003
2nd Impression 2008)

REGIONAL GEOCHEMICAL DISPERSION IN MATERIALS ASSOCIATED WITH ACID SULFATE SOILS IN RELATION TO BASE-METAL MINERALISATION OF THE KANMANTOO GROUP, MT TORRENS-STRATHALBYN REGION, EASTERN MT LOFTY RANGES, SOUTH AUSTRALIA.

M.S. Skwarnecki and R.W. Fitzpatrick

CRC LEME OPEN FILE REPORT 205

December 2008

(CRC LEME Restricted Report 185R, 2003
2nd Impression 2008)

CRC LEME is an unincorporated joint venture between CSIRO-Exploration & Mining, and Land & Water, The Australian National University, Curtin University of Technology, University of Adelaide, Geoscience Australia, Primary Industries and Resources SA, NSW Department of Primary Industries and Minerals Council of Australia.

Headquarters: CRC LEME c/o CSIRO Exploration and Mining, PO Box 1130, Bentley WA 6102, Australia

Electronic copies of the publication in PDF format can be downloaded from the CRC LEME website: http://crcleme.org.au/Pubs/OFRSindex.html. Information on this or other LEME publications can be obtained from http://crcleme.org.au.
Hard copies will be retained in the Australian National Library, the J. S. Battye Library of West Australian History, and the CSIRO Library at the Australian Resources Research Centre, Kensington, Western Australia.

Reference:
Skwarnecki, M.S. and Fitzpatrick, R.W. 2003. Regional geochemical dispersion in materials associated with acid sulfate soils in relation to base-metal mineralisation of the Kanmantoo Group, Mt Torrens-Strathalbyn region, eastern Mt Lofty Ranges, South Australia. CRC LEME Restricted Report 185R, 193 pp. (Reissued as Open File Report 205, CRC LEME, Perth, 2008).

Keywords: 1. Regolith materials 2. Geomorphology - Victoria 3. Salinity 4. River Murray

ISSN 1329-4768
ISBN 978 0 643 09675 2

Addresses and affiliations of Authors:

M.S. Skwarnecki and R.W. Fitzpatrick
CSIRO Land and Water
Private Bag 2
GLEN OSMOND
SA 5064

Published by: CRC LEME
c/o CSIRO Exploration and Mining
PO Box 1130, Bentley, Western Australia 6102.

PREFACE

Iron- and S-rich precipitates from rising ground and surface waters (bearing sulfate and Fe^{2+} ions) accumulate in saline springs, seeps, wetlands and creeks in the Mount Lofty Ranges. These materials may scavenge anomalous concentrations of elements such as Cu, Pb, Zn, which have been sourced from mineralized zones in bedrock, and hence represent a good sample medium for mineral exploration.

This regional geochemical survey of part of the eastern Mount Lofty Ranges corroborates the findings of the previous orientation study at Mount Torrens and demonstrates that the sampling of acid sulfate soils is a valid geochemical sampling medium. Not only are anomalous concentrations of Ag, As, Au, Bi, Cd, Co, Cu, Hg, In, Mo, Ni, Pb, Sb, Se, Tl and Zn indicative of mineralization in these sulfidic materials, but this study also documents the presence of new generations of sphalerite, galena, chalcopyrite, native gold and Mn oxides, precipitated by biomineralization processes.

CONTENTS

LIST OF FIGURES

LIST OF TABLES

LIST OF APPENDICES

Page

ABSTRACT

Acid sulfate soils (ASS) from creeks, dams, seeps, springs and wetlands were sampled in an area 25 x 40 km in the eastern Mount Lofty Ranges, between Mount Torrens in the north and Strathalbyn in the south. Acid sulfate soils are common in landscapes with relief and can occur in seeps or springs (on mid to upper slopes of valleys) or in creeks and wetlands, typically in narrow valleys. Acid sulfate soils contain sulfidic materials (Fe and other sulfides; pH >4), which may form continuous layers (up to 30 cm thick), or consist of a series of discontinuous layers, normally below water level, associated with decaying vegetation and algae. Acid sulfate soils appear to be absent from broad valleys, which contain relatively thick accumulations of alluvium and where drainages may be ephemeral.

Sulfidic materials may contain two types of iron sulfide: pyrite and Fe monosulfides (such as greigite or mackinawite). The matrix to the sulfides is dominantly quartz, with variable minor amounts of mica, plagioclase, potash feldspar, calcite and kaolinite. In drained or disturbed ASS, several rare to accessory phases such as gypsum, halite, jarosites, ferrihydrite and/or schwertmannite and Fe oxides occur in sulfuric horizons (pH <4). However, in the vicinity of mineralized zones in bedrock, sulfidic materials may also contain sphalerite, galena, chalcopyrite, native gold, barite and Mn oxides (with minor Co, Zn and I). These minerals tend to be intimately associated with, and incorporated in, organic matter. In particular, sphalerite and galena tend to occur in very fine (<1 μm diameter) spherical grains and have been precipitated as a result of biomineralization. The compositions of the sphalerites in sulfidic material are relatively Fe-poor, in contrast to the relatively Fe-rich sphalerite from the nearby primary mineralized zones.

Acid sulfate soils proximal to mineralized zones in bedrock are anomalous in a range of elements, including Ag, As, Au, Bi, Cd, Co, Cu, Hg, In, Ni, Mo, Pb, Sb, Se, Tl and Zn, for example, at Wheal Ellen, Glenalbyn, the Mt Torrens and Monarto prospects, and in the Kanmantoo area. Several anomalies also occur in locations not associated with known mineralization. These materials may also record geochemical differences in parent bedrock, such as Na and K being positively correlated to the west of the Bremer Fault, but are negatively correlated and have greater absolute Na contents to the east of the fault. These differences may relate to regional fluid flows, possibly related to the relatively intense mineralizing event to the west of the fault, or to regional metamorphism, or to granitoid intrusion in the east. A soil-landscape model has been developed for the soil, regolith and hydrogeochemical processes and explains geochemical dispersion from mineralized zones into acid sulfate soil seeps.

Surface waters, collected at many of the acid sulfate soil sample sites, vary considerably in composition from non-saline to extremely saline, and from weakly acidic to alkaline. Values of electrical conductivity (EC) closely follow concentrations of Na^+, K^+, Ca^{2+}, Mg^{2+} and SO_4^{2-} ions.

Thus this study confirms that acid sulfate soils are a new sampling medium for mineral exploration.

1. REGIONAL SETTING

1.1 Introduction

Acid sulfate soils in saline seeps occur naturally in the Mount Lofty Ranges, but their area is increasing in response to land clearing, rising water tables and soil disturbance (such as drainage, or pugging by grazing animals). The seeps can form unsightly discharge areas, with eroded “iron ochre scalds” and swampy saline sulfidic soils, which continue to creep up slopes in high rainfall (>500mm) catchments. Recent investigations have found that accumulation and oxidation of iron and sulfur in seasonally rising ground and surface water are causing less permeable soil layers to form in discharge areas (Fitzpatrick et al., 1992, 1996). Data on the composition of the iron oxide precipitates forming in the saline sulfidic soils indicates that they commonly have elevated levels of indicator elements, for which the iron oxides have a high sorptive capacity (Skwarnecki et al., 2002a). These scalds and associated iron oxide precipitates thus have potential as a geochemical sampling medium for the detection of mineral deposits. In particular, they have potential to give, or at least enhance, surface expressions of otherwise buried and blind deposits.

In several catchments in the Mount Lofty Ranges, saline groundwater, enriched in sulfate (SO_4^{2-}) and ions such as Na^+, Mg^{2+}, AsO_4^{3-}, I^- and Cl^-, can seep up through the soil and concentrate by evaporation, forming various mineral precipitates within and on top of the soil. The combination of rising sulfate-rich groundwater tables, waterlogging, agricultural activity and fractured lithologies rich in Fe and S can lead to the formation of saline soils with potential and actual acid sulfate (AASS) soil conditions (Fitzpatrick et al., 1996, 2000). If the soil is waterlogged, anaerobic bacteria use the sulfate to promote the degradation of organic matter. This process produces pyrite (FeS_2) and forms "sulfidic materials". These pyrite-enriched soils are termed "potential" acid sulfate soils (PASS) because they have all the ingredients necessary to produce AASS. AASS result when cattle, drainage works or other disruptions expose the pyrite, within waterlogged soils, to air. When this happens, pyrite is oxidized to sulfuric acid and various iron sulfate-rich minerals precipitate, and "actual" ASS forms. When sulfuric acid forms, the soil pH can drop from neutral (pH 7) to below 4, with values as low as 2, to form a "sulfuric horizon". The sulfuric acid dissolves layer-silicate minerals within the soil, causing ions (e.g., Na^+, Mg^{2+}, Ca^{2+}, Ba^{2+}, Cl^-, SO_4^{2-}, SiO_4^{4-}) to be mobilized on the soil surface and in stream waters.

An orientation study at the Mount Torrens Pb-Zn prospect (Skwarnecki et al., 2002a, b) indicated that saline acid sulfate seeps and soils can be used as exploration sampling media. Sulfidic materials locally contain anomalous concentrations of As, Ba, Bi, Cd, Cu, P, Pb, Sn, Tl and Zn. That study concluded that these sulfidic materials and associated iron oxide precipitates were a geochemical sampling medium for the detection of mineral deposits. The next stage of the project, the regional sampling of seeps, constrained by catchments and areas of known mineralization, together with background areas with no known mineralization, to provide a robust evaluation of the technique, is the subject of this report. Interestingly, during the project planning of this next stage of work Dr CRM Butt noted the similarities between the Inland Acid Sulfate Soils previously identified in the Mount Lofty Ranges (e.g. Fitzpatrick et al., 1992, 1996; Skwarnecki et al., 2002a, b) and “iron oxide seepages” in Northern Island (Butt and Nichol 1979). Both types are bacterial, metal-rich and the result of land-use change. In Northern Island, the seeps also give surface expression to otherwise concealed mineralization.

1.2 Location, landscape, climate and land use

Samples were collected in the eastern Mount Lofty Ranges (Figure 1.1) from an area 1000 km^2 between Mt Torrens (34°53'S 138°58'E) and Palmer (34°51'S 139°09'E) in the north and Strathalbyn (35°16'S 138°54'E) in the south.

The landscape is undulating low hills with altitudes between 400 to 500 m and local relief of about 30 to 50 m. The climate of the area is Mediterranean, with a pronounced maximum of rainfall in winter (May to August) and hot, dry summers (December to February). Annual rainfall is topographically controlled, with a mean average annual rainfall of 680 mm. Average annual rainfall varies from about 800 mm at Mount Torrens and Mount Barker (in the northwest), to about 500 mm at Strathalbyn, 420 mm at Palmer, and to 400 mm and less south-east of Callington (in the southeast). During the sampling period (July-August, 2002), rainfall was significantly below average (97 mm at Mt Torrens (average 150 mm) and 76 mm at Strathalbyn (average 104 mm).

The land cover of the area is predominantly pasture, with most native tree vegetation having been cleared by the end of the 19th century. The remaining areas of remnant vegetation are associated mainly with topographic high points, roadways and watercourses. Land use is predominantly grazing by sheep or cattle. Increasingly, land is being used for more intensive purposes such as viticulture, commercial forestry and some cereal cropping. The catchments drain to the east and into the Murray River system. Stream channels have a normal tributary pattern and are mostly eroding residual soils, bedrock or the alluvial soils and sediments of valley floors, locally to depths of two to three metres.

1.3 Regional geology

The Kanmantoo Group (Figure 1.2; Belperio et al., 1998; Toteff, 1999) occurs in a fault-controlled basin that developed in the early Cambrian by extensional tectonism along the southeastern flank of the Neoproterozoic Adelaide Geosyncline, following initial stable platform carbonate sedimentation (Normanville Group). The marine clastic flyschoid sediments of the basin (together with the Neoproterozoic succession to the west) were deformed, metamorphosed and intruded by granites during the Delamerian Orogeny (middle to late Cambrian), and are now exposed in an arcuate zone over 300 km in length in the eastern and southern Mount Lofty Ranges. At least two main phases of deformation have been recognized. Metamorphism at low pressure and high temperature locally attained amphibolite facies, and appears to have coincided with a major period of granite emplacement.

The apparent thickness of the Kanmantoo Group is up to 15 km, and may consist of a stack of thrust sheets. The main rock types are sandstones, siltstones and phyllites, with intercalated pelites and minor carbonates. The lowermost sequence comprizes muddy sandstone and siltstone (Carrickalinga Head Formation), which passes up into cleaner, cross-bedded, feldspathic sandstone (Backstairs Passage Formation). A disconformity separates the Backstairs Passage Formation from the overlying upper parts of the sequence, which comprizes interbedded muddy sandstone and siltstone (Tapanappa and Balquhidder Formations), and dominantly fine-grained clastic rocks of the Talisker Calc-siltstone, and Tunkalilla Formation.

Most of the significant base metal syn-sedimentary mineralization in the Kanmantoo Group is confined to the Tapanappa Formation. It may be spatially associated with exhalites, such as garnetiferous lithologies (including BIF) and gahnite-bearing rocks, and unusual metamorphic

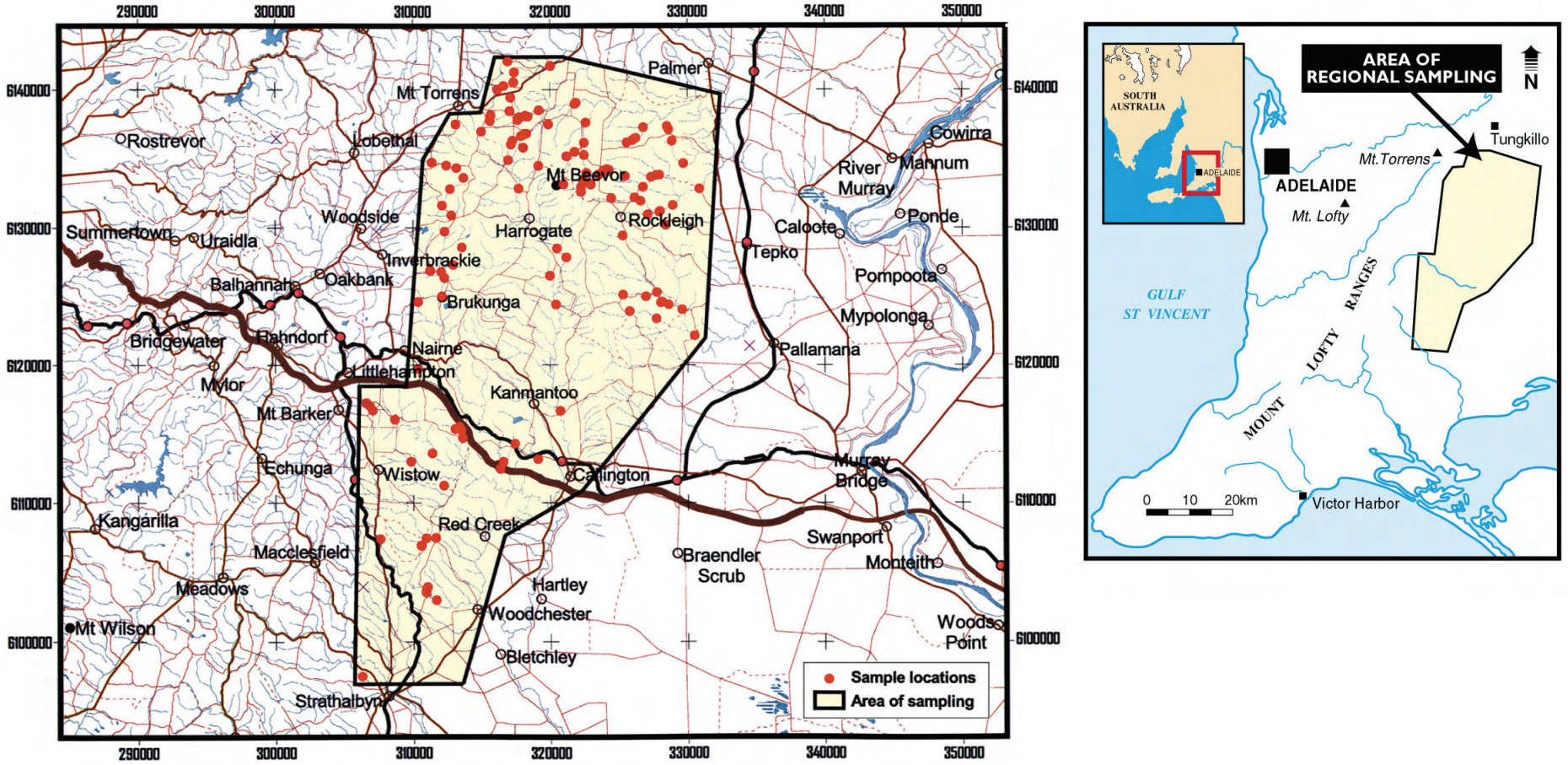

Figure 1.1. Location of the samples collected in the eastern Mount Lofty Ranges, South Australia.

mineral assemblages interpreted to be metamorphosed alteration zones. Sulfide mineralization has been classified into four commodity-based categories:

(i) Cu±Au (e.g., Kanmantoo (Both, 1990), Breadalbane, Bremer (Spry, 1976; Both, 1990));
(ii) Pb-Zn-Ag±Au (e.g., Aclare (Askins, 1968), Wheal Ellen (Wade & Cochrane, 1952; Spry, 1976));
(iii) Cu-As±Au (e.g., Preamimma (Anon., 1924), Glenalbyn (Brown, 1908));
(iv) Fe (pyrite, pyrrhotite) at various stratigraphic levels (e.g., Brukunga (George, 1967)).

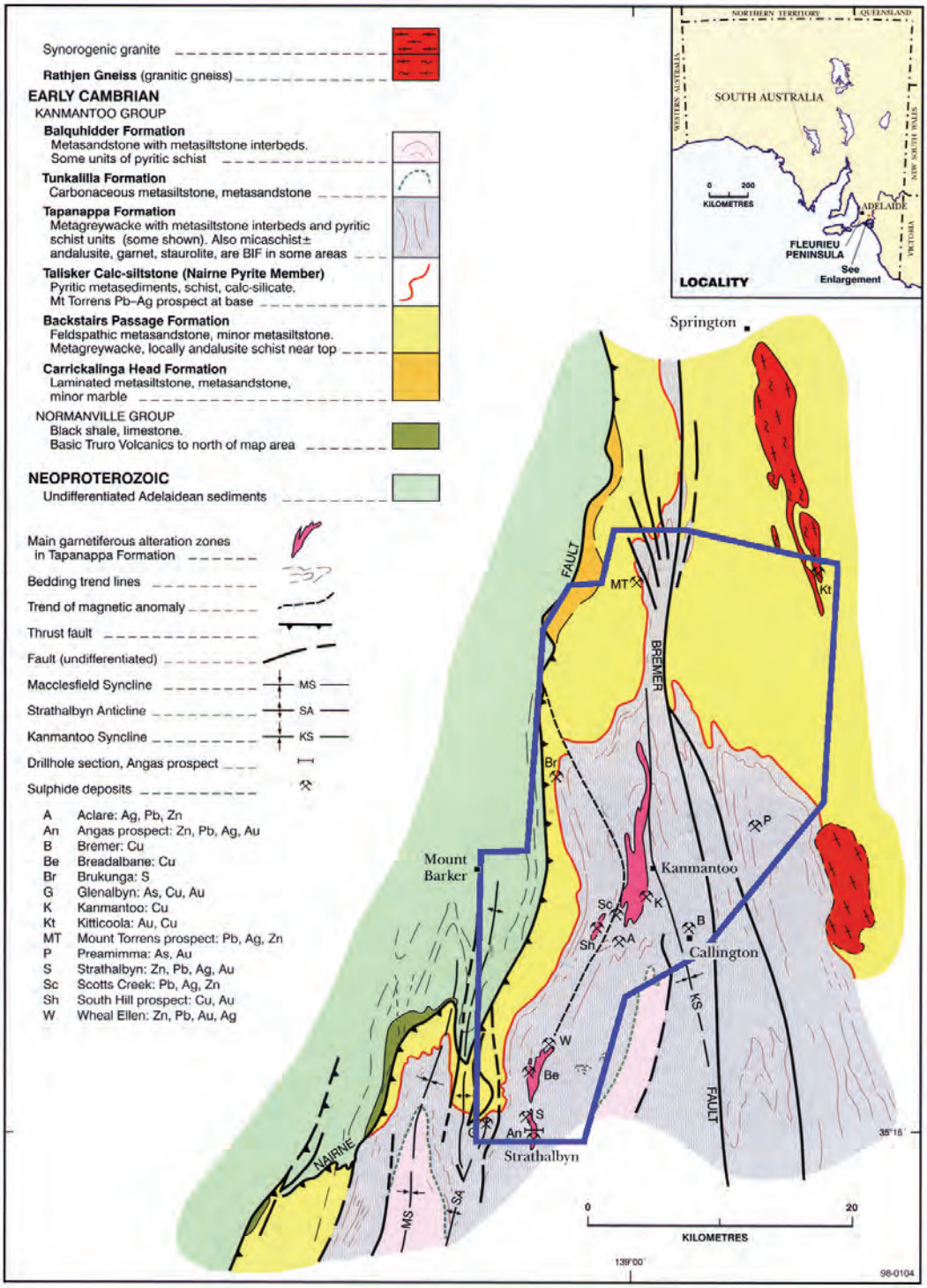

Figure 1.2. Regional geological setting of mineral deposits in the Kanmantoo Group (from Toteff, 1999). The blue polygon indicates the area of study.

1.4 Objectives and work programme

The principal objective was to determine whether the regional geochemistry of saline ASS and seeps would reflect the incidence of base metal mineralization in the Kanmantoo Group. Specific objectives included:

(i) determination of the geochemistry of sulfidic materials and sulfuric horizons from ASS and saline seeps;
(ii) determination of the mineralogical expressions of anomalous geochemistry in ASS and seeps;
(iii) evaluation of the geochemistry of surface waters (from creeks, seeps, wetlands and dams) and implications for soil and water salinity.

The main part of the regional sampling programme was carried out between late June and early September, 2002, during a relatively dry winter. Previous samples from acid sulfate seeps at the Mount Torrens prospect (Skwarnecki et al., 2002a) were incorporated into this study.

2. STUDY METHODS

2.1 Collection of soil and water samples

One hundred and fifty samples of ASS materials were collected (Figure 2.1), of which 125 were sulfidic, and 25 were oxidized:

(i) 35 samples from **seeps** (8 oxidized);
(ii) 71 samples from **creeks** (9 oxidized);
(iii) 7 samples from **wetlands** (3 oxidized);
(iv) 6 samples from **springs** (1 oxidized);
(v) 6 samples from **dams**;
(vi) 4 samples from **creek banks**;
(vii) 2 (oxidized) samples from **scalds**;
(viii) 2 (oxidized) samples from water-filled **depressions**.

Sixteen samples from Mt Torrens were included (Skwarnecki et al., 2002a), comprising 6 from creek banks, 6 from wetlands, 2 from seeps and 1 each from a spring and a creek.

One hundred and two water samples were collected (Figure 2.2):

(i) 68 samples from **creeks**;
(ii) 12 samples from **seeps**;
(iii) 9 samples from **springs**;
(iv) 8 samples from **dams**;
(v) 5 samples from **wetlands**.

Water samples were collected in plastic 50 ml centrifuge tubes (with lids), taking care, where possible, to avoid contamination from sediment or ferrihydrite precipitates.

2.2 Sample preparation

In the laboratory, samples were oven-dried at 40^{o}C. A 200 g aliquot of sample was split and was milled (by AMDEL in Adelaide) in a Cr-free disc mill to a nominal 90% passing

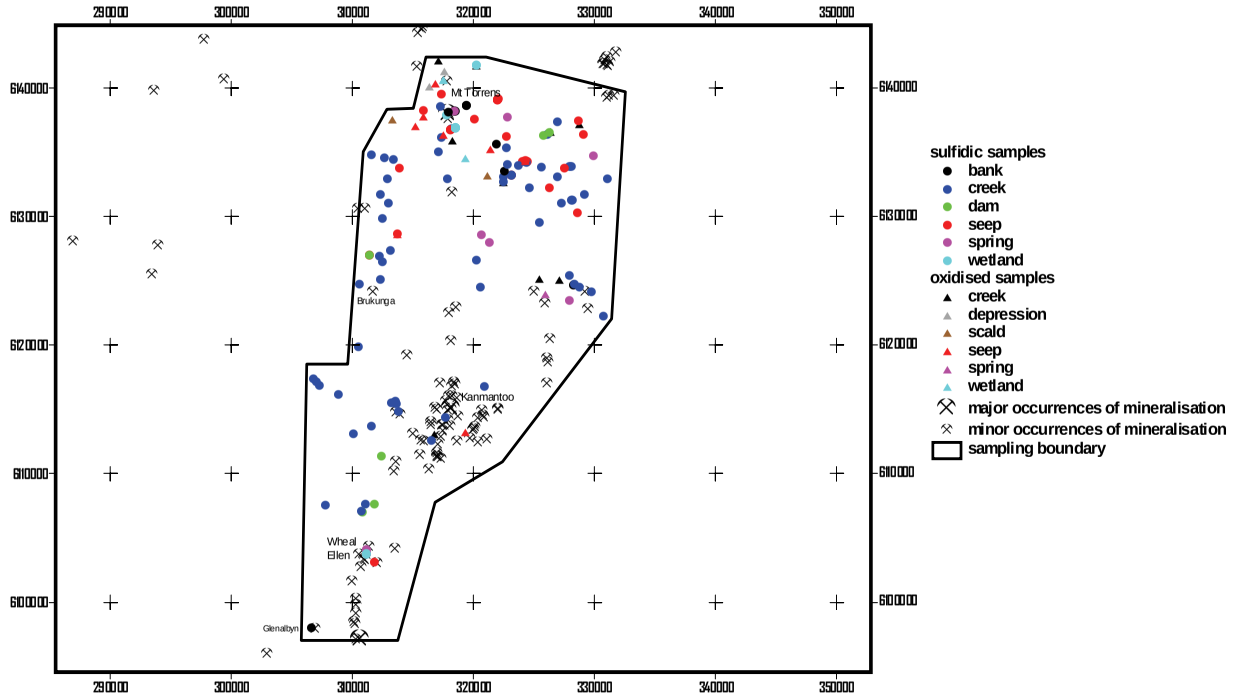

Figure 2.1. Locations of samples from ASS and their provenance.

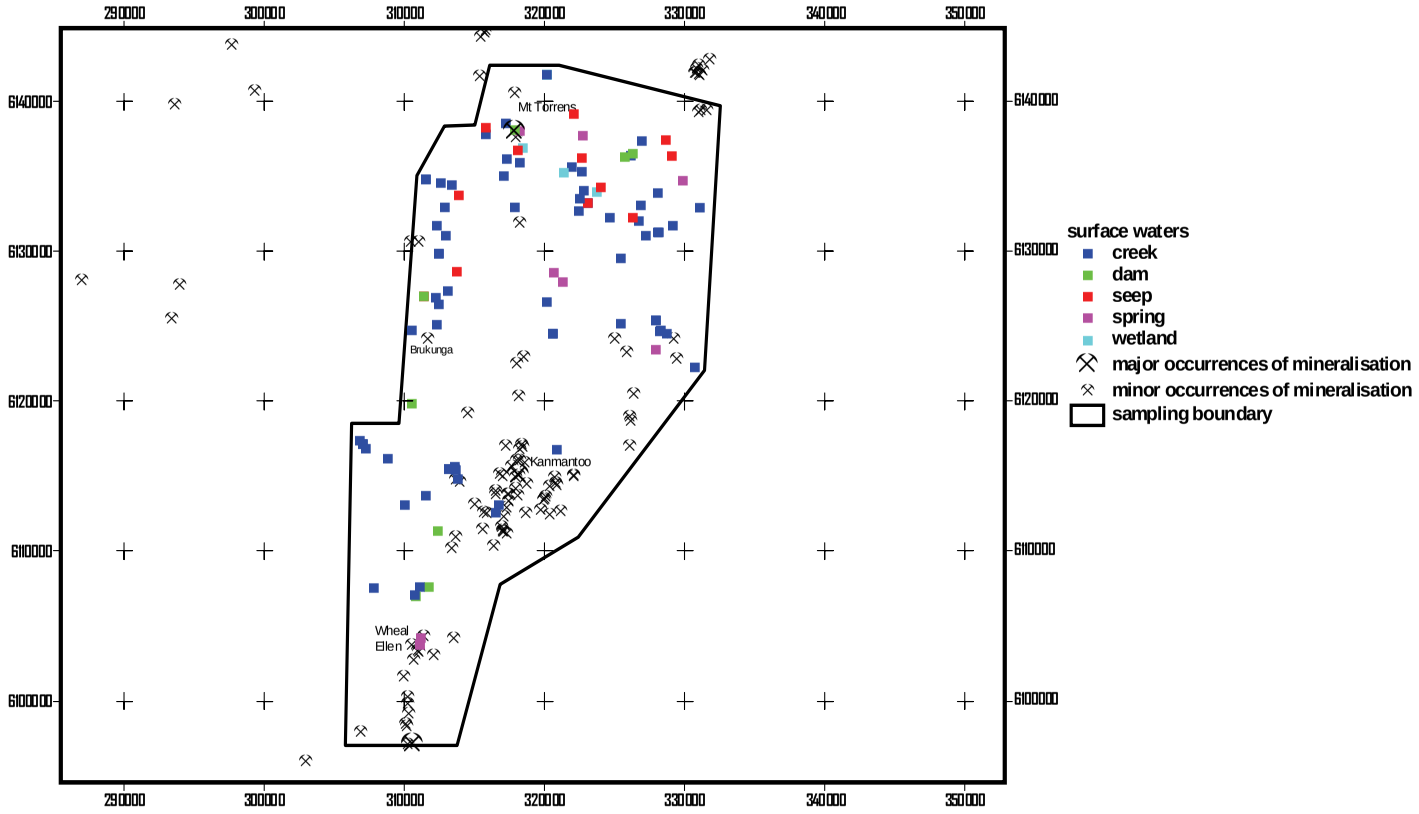

Figure 2.2. Surface water sample locations and their provenance. Samples were centrifuged and/or filtered through a 45 μm filter only if there was suspended material in the solution.

through 106 μm. A 10 ml aliquot of water sample was extracted from the centrifuge tubes and was presented to the ICP-OES. If analyte concentrations were outside the upper range of the calibration, they were repeated after dilution.

2.3 Analysis

The ground samples were analysed by atomic absorption spectrophotometry (AAS), inductively coupled plasma optical emission spectrometry (ICP-OES) and inductively coupled plasma spectrometry (ICP-MS) by AMDEL in Adelaide. The digestions, methods and respective element suites were:

(i) Au – aqua regia digest (a mixture of nitric and hydrochloric acids) of sample (up to 50 g), extraction into di-isobutyl ketone (DIBK), and analysis on a graphite furnace AAS;
(ii) ICP-OES suite (Al, Ba, Ca, Cr, Cu, Fe, K, Mg, Mn, Na, Nb, Ni, P, Pb, S, Ti, V, Zn); sample digestion with hydrochloric, nitric and hydrofluoric acids, with a final dissolution in hydrochloric acid (mixed acid digest);
(iii) ICP-MS suite (Ag, As, Bi, Cd, Co, Cs, Ga, In, Mo, Rb, Sb, Se, Sn, Sr, Te, Th, Tl, U, W, Y, Hf, Ce, Dy, Er, Eu, Gd, Ho, La, Lu, Nd, Pr, Sm, Tb, Tm, Yb); mixed acid digest;
(iv) Hg – aqua regia digest followed by generation of cold vapour and analysis by AAS.

The analytical data are listed in Appendix 1.

Water samples were analysed by ICP-OES for Al, B, Ca, Cu, Fe, K, Mg, Mn, Na, P, S, Si, Sr and Zn. The electrical conductivity (EC) and pH of each solution were also measured in the laboratory. The analyses are listed in Appendix 5.

2.4 Standards and statistical treatment of data

Pulped in-house rock standards (CRC LEME Standards 7, 9 and 10) were placed in the analytical stream to monitor precision. Results are given in Appendix 2. The recommended values were obtained from XRF and instrumental neutron activation analysis (INAA) data (reliable total analyses). The results obtained by ICP should not be compared too closely in absolute terms, since the mixed acid digests do not provide total element extractions and consequently element abundances are understated.

Statistical summaries of analytical data are provided Appendices 4 and 7. The intervals for the geochemical plots in Appendices 3 and 6 were determined from probability plots. Spearman Rank correlation coefficients were computed using DataDesk (version 6).

3. ACID SULFATE SOILS

3.1 Occurrence

Soils with acid sulfate features (such as Fe sulfide-rich material, or sulfuric horizons) occur in creeks, seeps, wetlands, springs and dams (Figure 2.1). With the exception of springs, acid sulfate soils tend to occur in those environments affected by salinity, such as: degraded agricultural land, commonly with tall wheat grass or sea-barley grass, adjacent to drainages; scalded ground, generally devoid of vegetation and dissected by erosion gullies; white salt encrustations along creek banks; or clear waters in creeks and dams (due to suppression of clay flocculation). Springs can occur in both saline and non-saline environments.

Acid sulfate soils are most common in landscapes with moderate relief, and can occur along creeks (Figures 3.1 and 3.2) or the sides of valley slopes (in seeps or springs; Figures 3.3 and 3.4) and in wetlands, typically where drainages are narrow, where there is abundant outcrop (i.e., in erosional terrains), and where drainages are flowing (such as Loxton Creek, about 25 km east of Mt Torrens).

In creeks, acid sulfate soils generally occur below water level, in upper parts of the stream sediment. The sulfidic horizons (continuous layers or as series of discontinuous layers and streaks) may in rare

Figure 3.1. Subsurface acid sulfate soil (grey to black) in stream sediment. Note that the sulfidic material occurs beneath a veneer of sand and the partial oxidation (orange-brown). Sample site KRS59.

Figure 3.2. Oxidized acid sulfate soil (red-brown to orange-brown) in dried-out pool along creek line. Sample site KRS70.

Figure 3.3. Acid sulfate soil in a natural spring associated with wetland vegetation. Sample site KRS142.

Figure 3.4. Acid sulfate soil in a seep in pasture. Sample site KRS135.

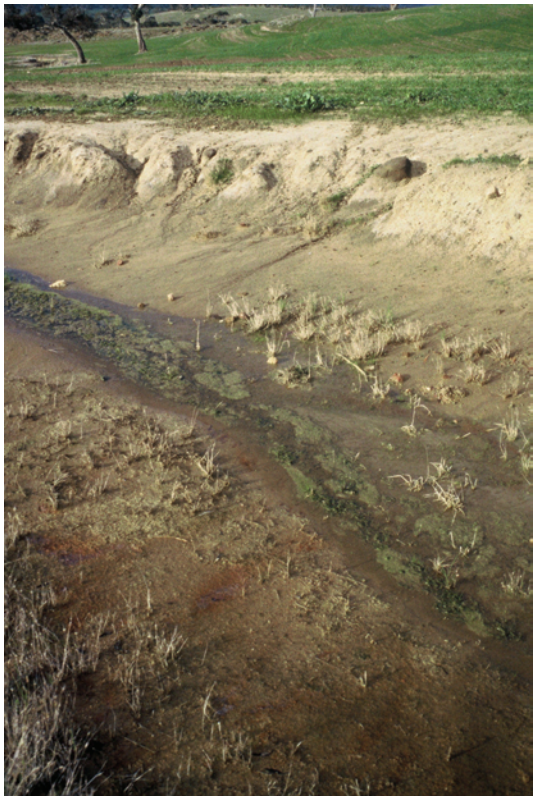

Figure 3.5. Ferrihydrite (orange-brown) weeps in stream sediment indicating the presence of sulfidic material beneath a veneer of sand. Sample site KRS68.

Figure 3.6. Ferrihydrite-rich layer (orange-brown) overlying sulfidic material. Sample site KRS63.

instances exceed 30 cm in thickness, and are commonly associated with decaying vegetation and green/pink algae, typically in stagnant pools. The presence of sulfidic materials in stream sediment may be indicated by ferrihydrite weeps (Figure 3.5), or, in extreme cases, by a layer several millimetres thick of ferrihydrite and orange algae (Figure 3.6). In contrast, acid sulfate soil features were not found where drainages are dry or along broad valleys with relatively thick alluvium (i.e., in depositional terrains), as in the area between Harrogate and Callington (Figure 1.1).

In a few instances, acid sulfate soil materials were found in dried-out, sandy creek beds, in damp depressions or below decaying algal mats, several centimetres below surface associated with subsurface water. Where desiccation was complete, the sulfidic material in the acid sulfate soil had been oxidized to red-brown/orange-brown Fe oxides (mainly ferrihydrite, schwertmannite or goethite; Figure 3.2) and occurred as layers mimicking the original sulfidic material in the acid soil layer.

There are two end-member types of sulfidic materials in acid sulfate soils, based on iron sulfide mineralogy: (a) pyrite-bearing material; and (b) Fe monosulfide-bearing material, containing Fe sulfides such as greigite or mackinawite (Bush & Sullivan, 1997). However, in practice, most, if not all, samples collected contain both. The two types can be distinguished in the field by smell (Fe monosulfide-bearing materials tend to be malodorous), colour (Fe monosulfide-rich materials are black and gelatinous, pyrite-rich materials tend to be brown), and chemical reaction with HCl (monosulfides react to produce H_2S, pyrite is unreactive).

3.2 Mineralogy

Acid sulfate soils are quartz-rich, with variable minor amounts of muscovite, plagioclase, orthoclase, microcline, calcite, sulfides (pyrite and/or monosulfides) and kaolinite, and lesser to accessory halite, bassanite ($CaSO_4.^1/_2H_2O$), gypsum, jarosite, natrojarosite, bischofite ($MgCl_2.6H_2O$), ferrihydrite and/or schwertmannite, hematite, goethite, aragonite, montmorillonite, illite, halloysite, beidellite, zircon, anatase and/or rutile, monazite, xenotime, ilmenite, actinolite, biotite and chlorite. In one sample, one grain of $CdCl_2$ (Figure 3.7) was associated with halite, within a ferrihydrite precipitate (Figure 3.8).

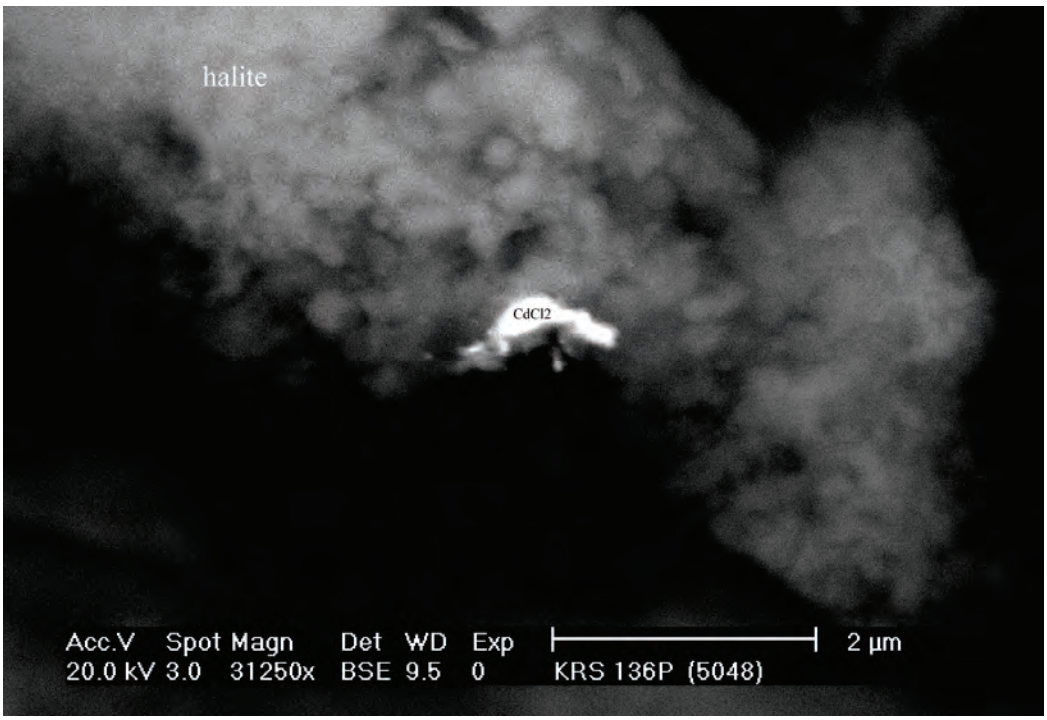

Figure 3.7. An anhedral grain of $CdCl_2$ (CdCl2) associated with halite from a ferrihydrite precipitate from a narrow gully high on the side of a hill, near Charleston Conservation Park. Sample KRS136P. Back-scattered electron image (SEM).

Figure 3.8. Ferrihydrite precipitate (orange-brown) in a small gully, near Charleston Conservation Park. Sample site KRS136.

Adjacent to mineralized zones in bedrock, acid sulfate soil materials may contain sulfides other than pyrite and monosulfides, such as sphalerite, galena and chalcopyrite, sulfates such as barite and plumbojarosite (see Skwarnecki et al., 2002a), native gold and Mn oxides (with minor Co, Zn and I). The presence of these minerals corresponds to anomalous accumulations of Cu, Pb, Zn, Au and other elements (see Section 4 below).

3.2.1. Sulfides

Pyrite

Pyrite is the most common sulfide. It occurs as:

(i) disseminated euhedral cubes, typically associated with organic matter (Figure 3.9);
(ii) individual framboids (Figure 3.10), or clusters of framboids (Figure 3.11), associated with disseminated pyrite. Three types of framboids have been recognized:

  (a) the most common, comprising aggregates of cubes (Figure 3.12);
  (b) aggregates of pyritohedra (Figure 3.13);
  (c) aggregates of rounded grains (Figure 3.14).

(iii) disseminated, in calcite nodules;
(iv) as coatings on organic matter (Figure 3.15), or on Mn oxides (Figure 3.16).

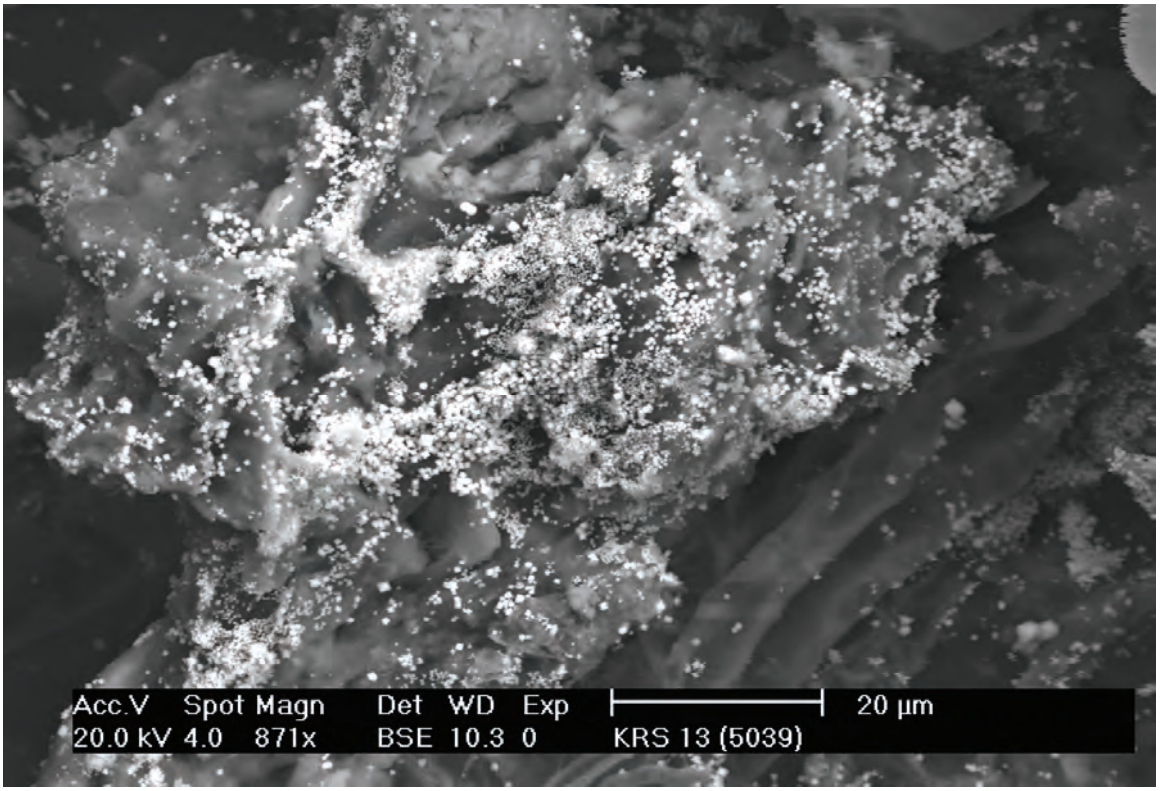

Figure 3.9. Fine-grained, disseminated pyrite grains on organic matter. Sample KRS13, mound springs at Wheal Ellen. Back-scattered electron image (SEM).

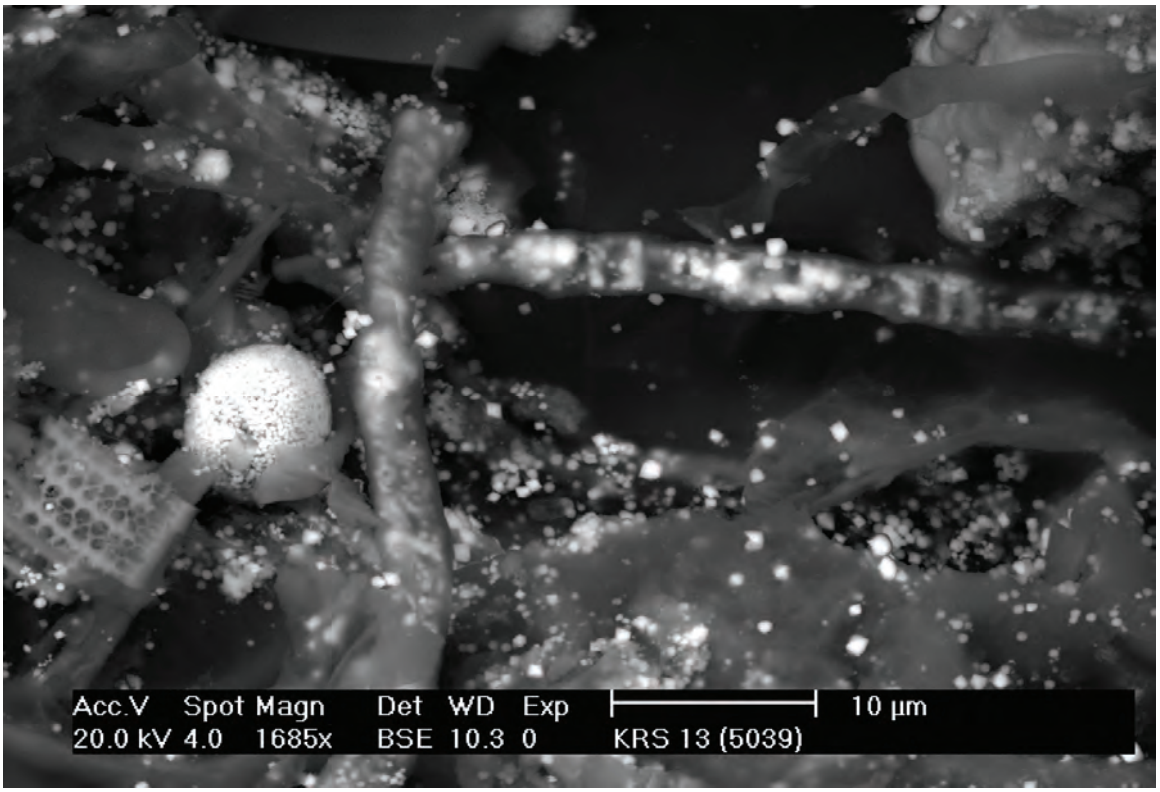

Figure 3.10. Pyrite framboid associated with a diatom fragment. The rootlets contain anhedral sphalerite grains. Sample KRS13, mound springs at Wheal Ellen. Back-scattered electron image (SEM).

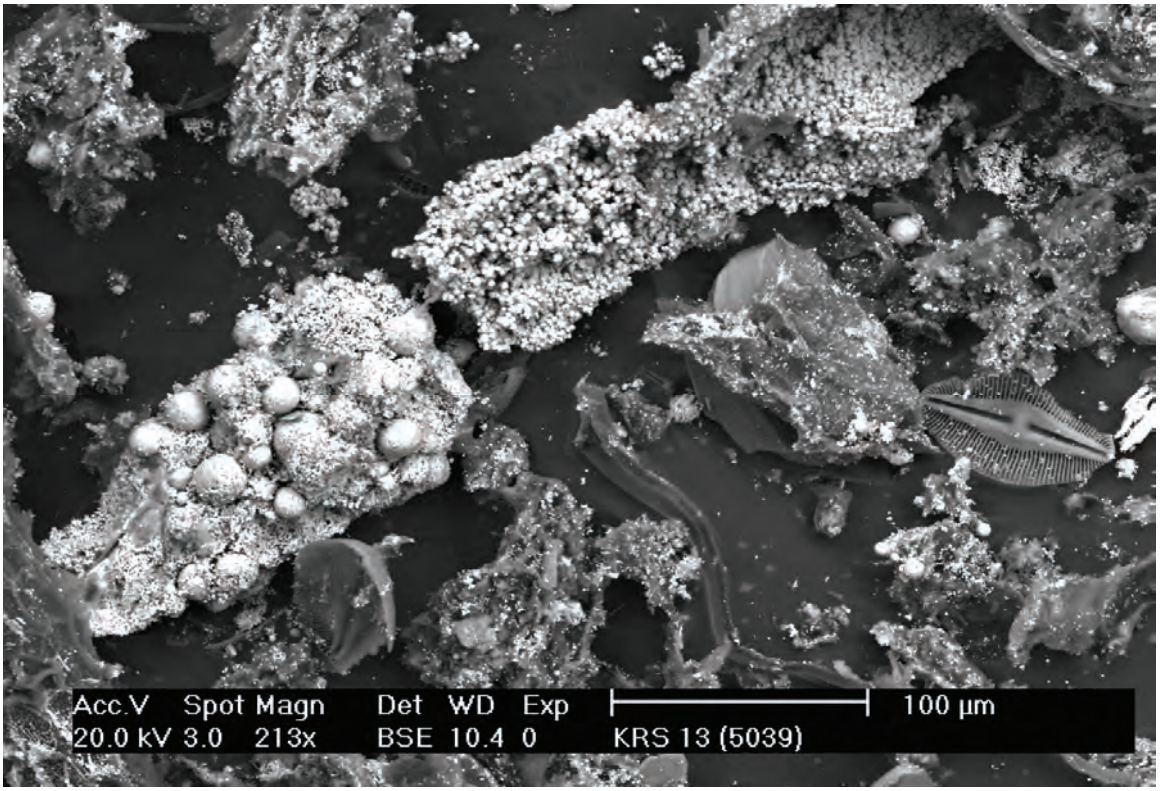

Figure 3.11. Aggregates of pyrite framboids and individual grains encrusting a rootlet. Individual framboids, disseminated pyrite cubes and rare diatoms occur in the matrix. Sample KRS13, mound springs, Wheal Ellen. Back-scattered electron image (SEM).

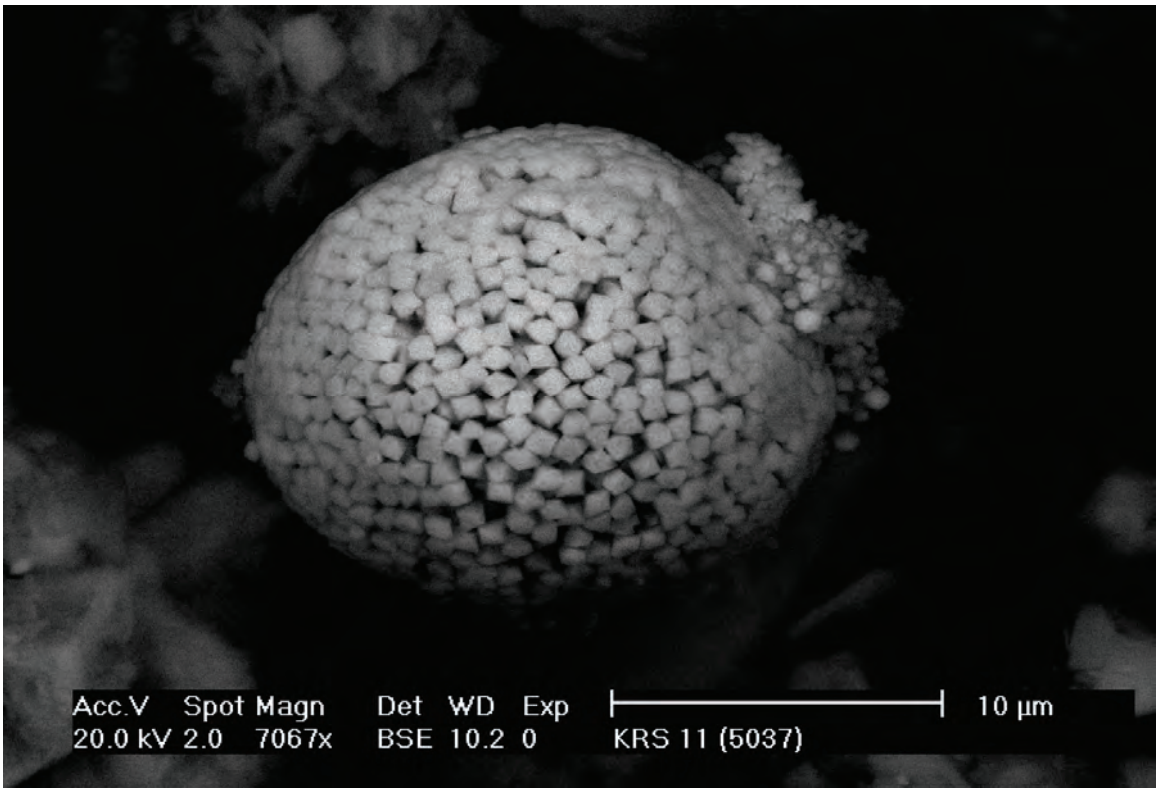

Figure 3.12. Pyrite framboid composed of cubes. Sample KRS11, Glenalbyn mine. Back-scattered electron image (SEM).

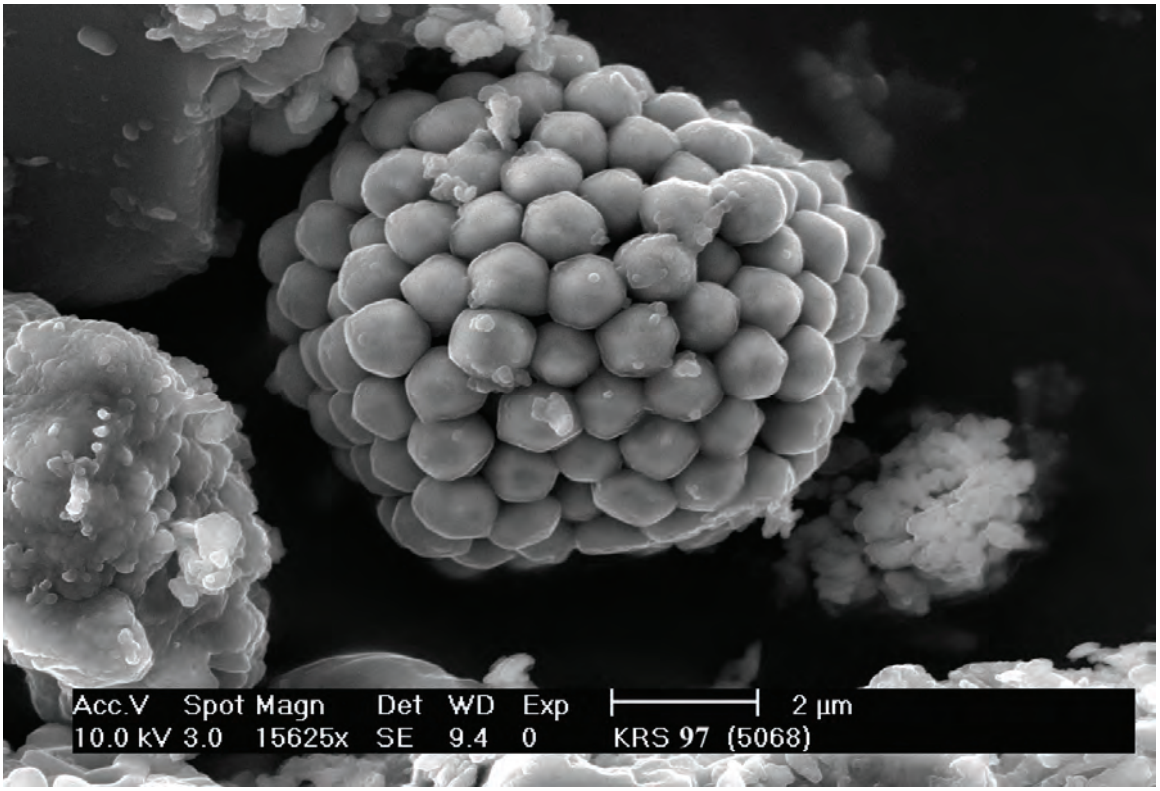

Figure 3.13. Pyrite framboid composed of pyritohedra. Sample KRS97. Back-scattered electon image (SEM).

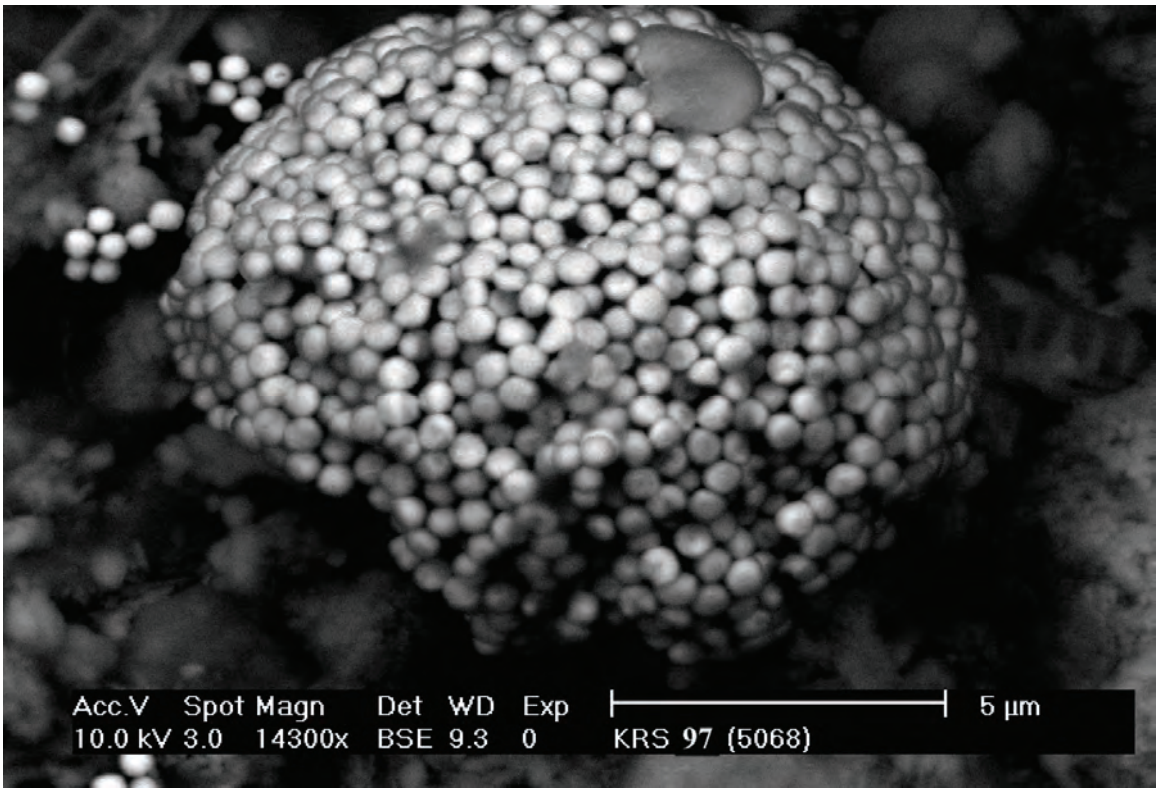

Figure 3.14. Pyrite framboid, with minor organic coatings, formed of rounded grains. Sample KRS97. Back-scattered electron image (SEM).

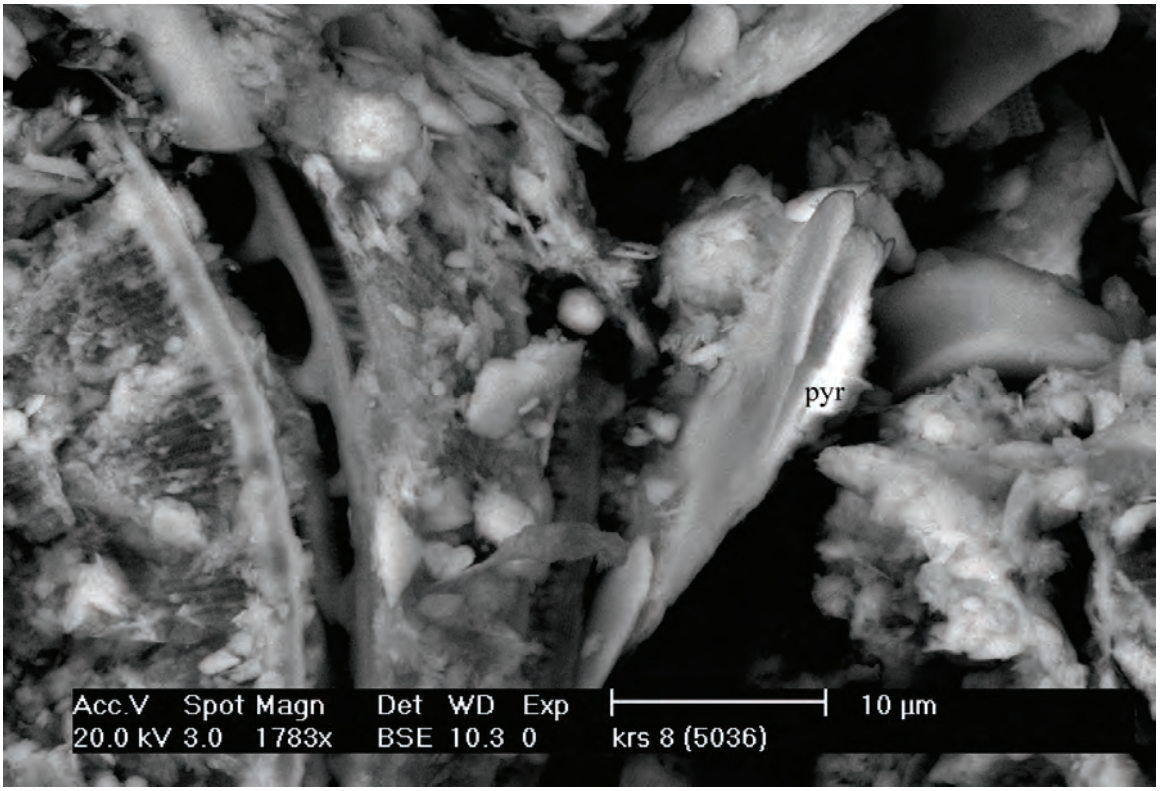

Figure 3.15. Partial pyrite (pyr) coating on organic matter. Sample KRS8. Back-scattered electron image (SEM).

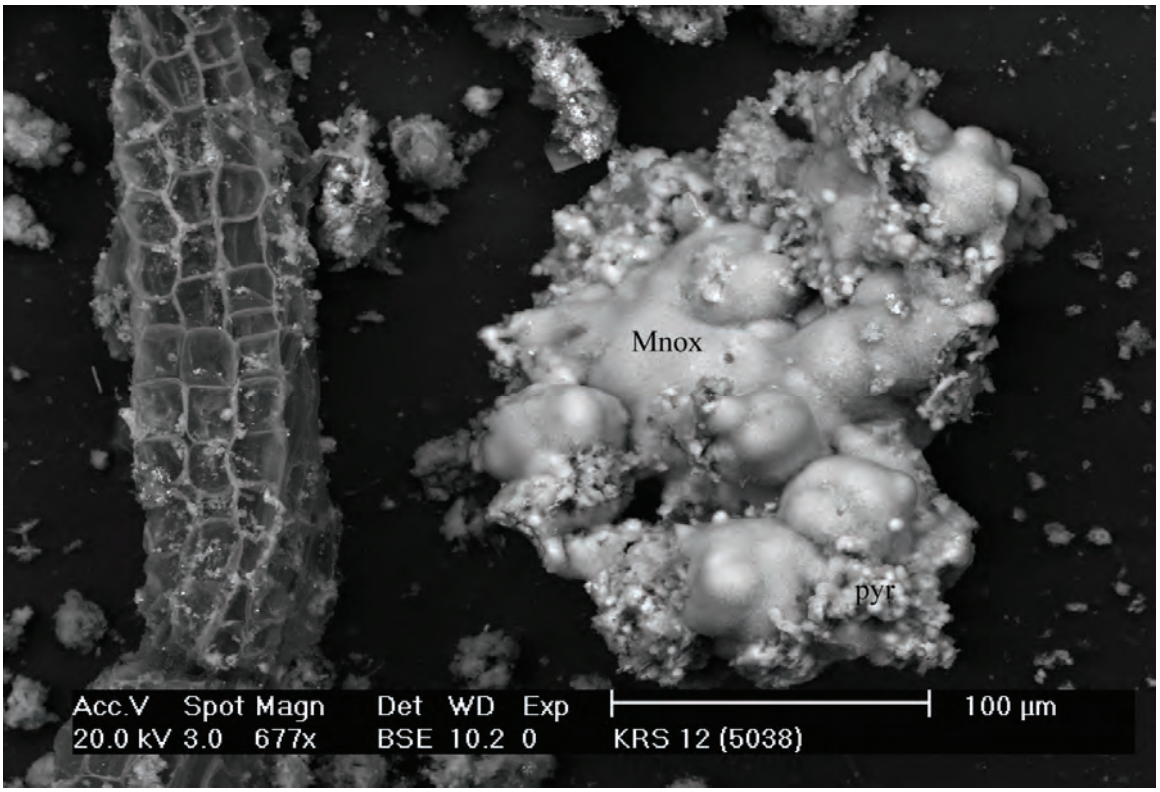

Figure 3.16. Pyrite (pyr) aggregates encrusting a botryoidal aggregate of cobaltian Mn oxides (Mnox) associated with plant material. Sample KRS12, mound springs at Wheal Ellen. Back-scattered electron image (SEM).

Iron monosulfides

Iron monosulfide grains (possibly greigite), with compositions ranging between $FeS_{1.18}$ and $FeS_{1.22}$, appear to be relatively rare, although field observations (colour, reaction with hydrochloric acid, smell) suggest that monosulfides should be more common than observed under the SEM. The reasons for this are unclear, but it is possible that most of the Fe monosulfide is very fine-grained (<<1 μm in diameter) and is unstable as soon as samples are freeze-dried. Iron monosulfide grains occur in pyritic materials as subhedra associated with Fe-Mn oxides (Figure 3.17), as corroded grains, or as irregular aggregates on organic matter (Figure 3.18).

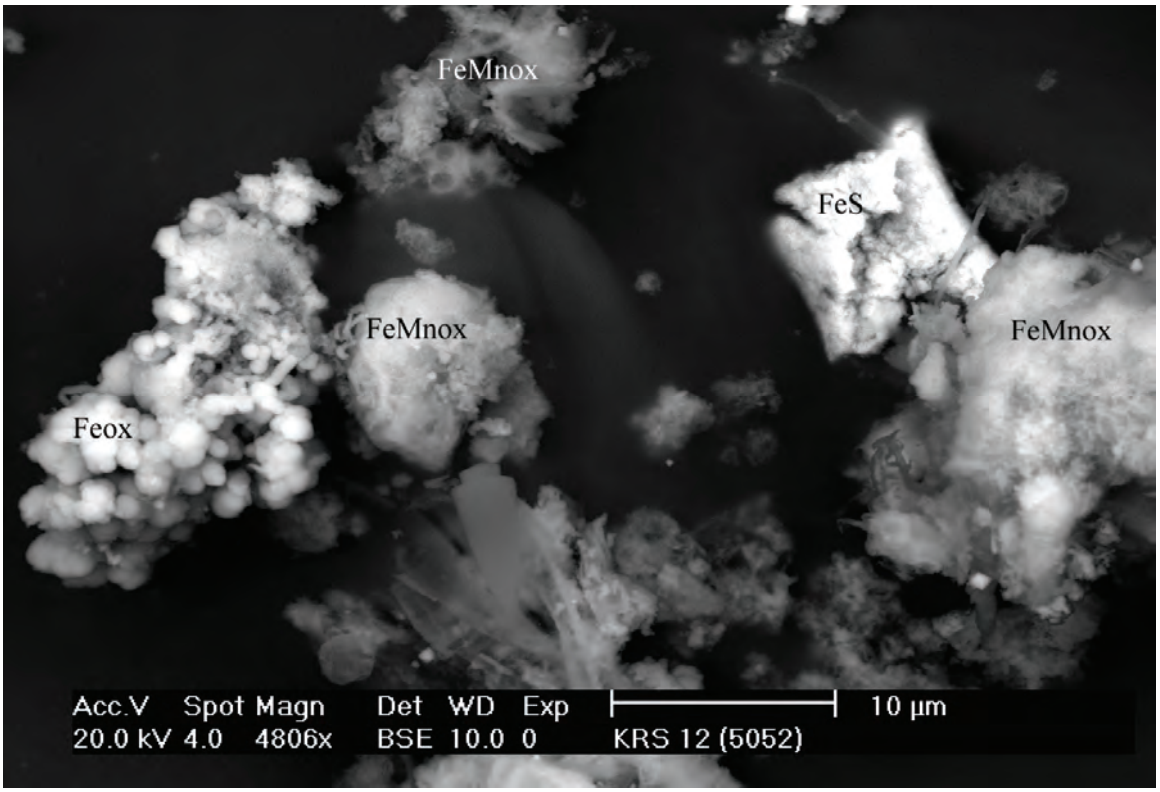

Figure 3.17. Subhedral grain of Fe monosulfide (FeS) associated with Fe-Mn oxide aggregates (FeMnox) and Fe oxides (Feox). Sample KRS12, mound springs at Wheal Ellen. Back-scattered electron image (SEM).

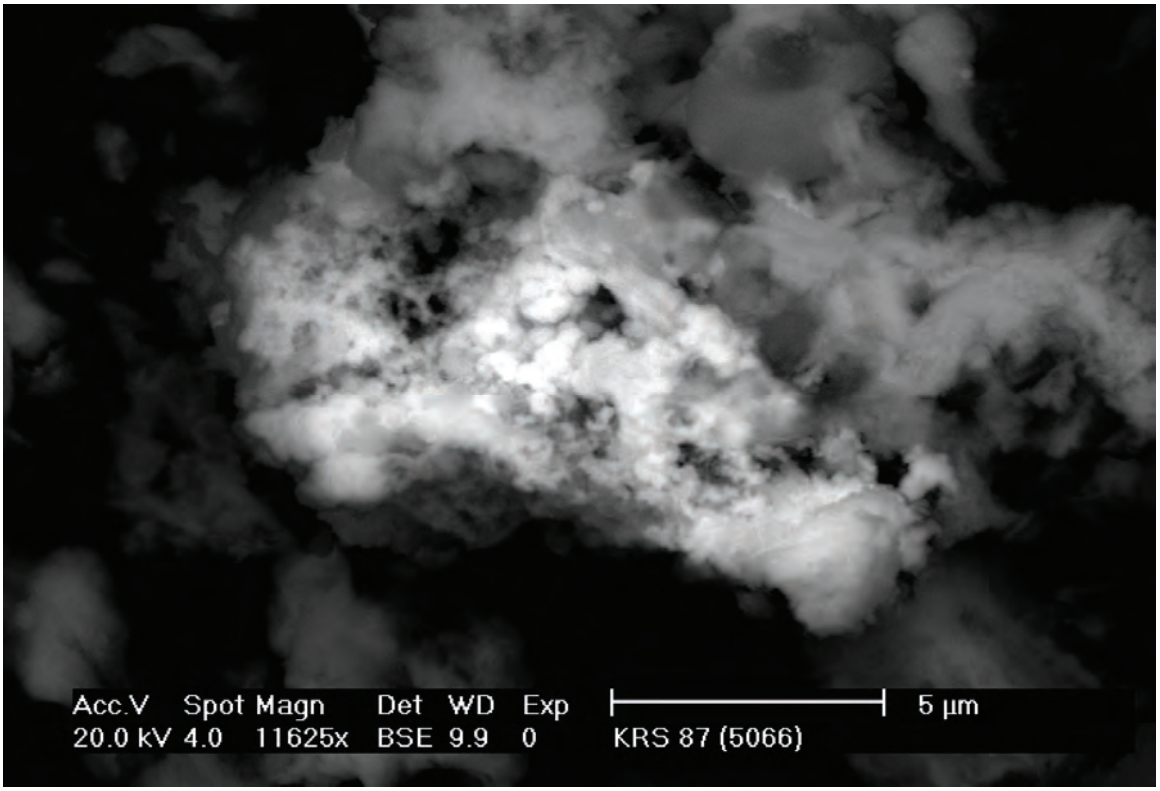

Figure 3.18. Aggregate of anhedral Fe monosulfide grains associated with kaolin and minor calcite. Sample KRS87. Back-scattered electron image (SEM).

Sphalerite

Sphalerite occurs in acid sulfate soils from mound springs at Wheal Ellen, the wetland along Rodwell Creek to the south of Wheal Ellen, and in a seep near an unnamed Cu-Au-Ag mine, south-east of Wheal Ellen. It is typically associated with pyrite, zincian Mn oxides and organic matter. The composition of sphalerite from the springs differs from that in the mineralized zones (Figure 3.19), in that sphalerite from the springs contains significantly less Fe.

Figure 3.19. Box plots showing compositional ranges for Fe in sphalerite from the mound springs and from the mineralized zone at Wheal Ellen. Data for sphalerite from mineralization taken from Spry (1976).

The most common forms of sphalerite are:

(i) spheres (up to 1 μm in diameter), generally as clusters on the surface of organic matter (Figure 3.20) or lining cell walls in plant material (Figure 3.21); the size of these spheres suggests that bacterial processes may have played an important role in their formation;
(ii) irregular flakes, with dissolution pits (Figure 3.22);
(iii) anhedral grains along plant rootlets (Figure 3.10), associated with pyrite framboids and cubes;
(iv) rounded grains, embedded in organic matter, associated with pyrite cubes (Figure 3.23);
(v) intergrowths with galena and clays;
(vi) as very fine-grained linear aggregates of sphalerite, pyrite and galena between plant cell walls (Figure 3.24).

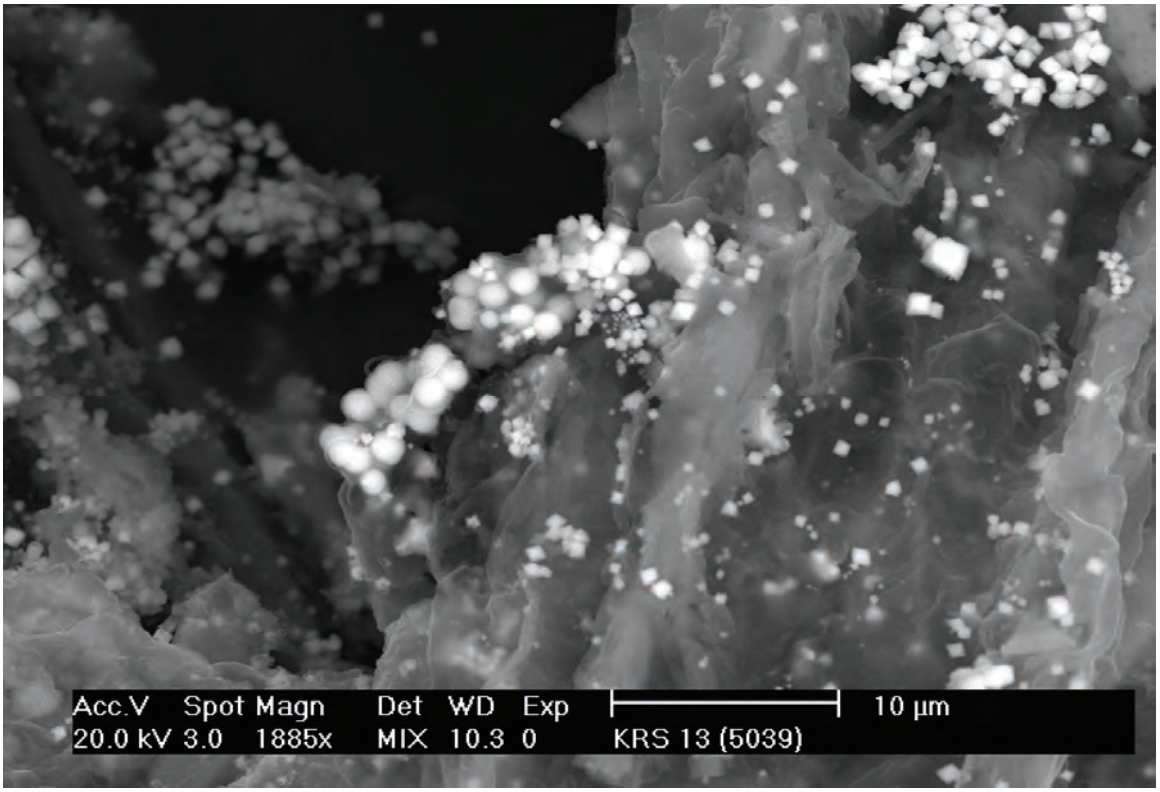

Figure 3.20. Aggregates of spherical sphalerite grains (centre) and pyrite cubes (top right) on organic matter. Sample KRS13, mound springs at Wheal Ellen. Back-scattered electron image (SEM).

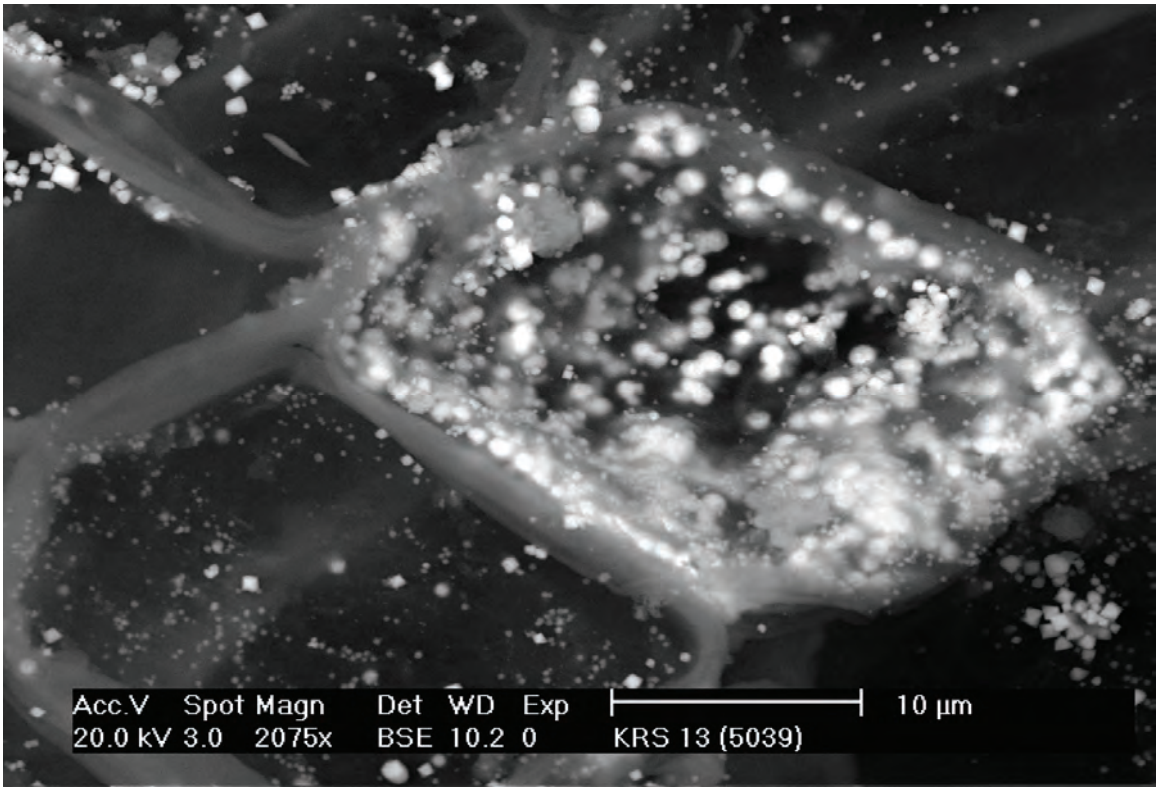

Figure 3.21. Spherical sphalerite grains lining plant cell walls. Sample KRS13, mound springs at Wheal Ellen. Back-scattered electron image (SEM).

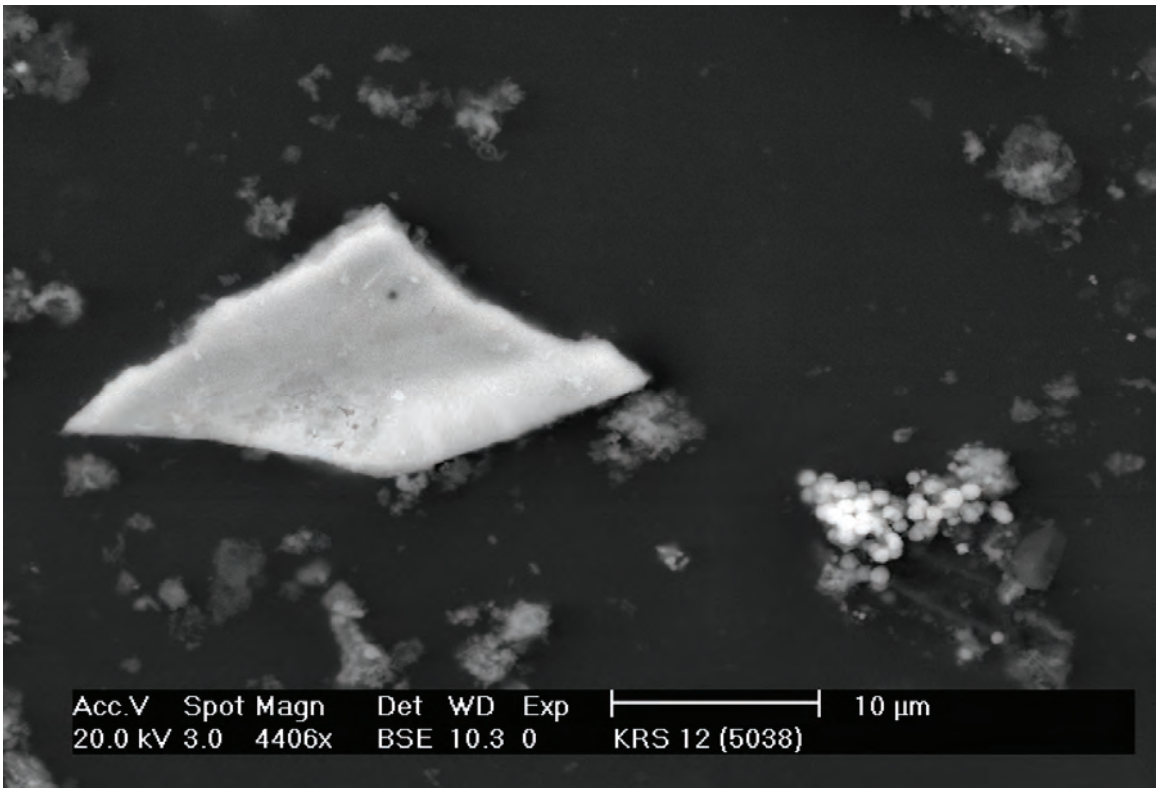

Figure 3.22. Sphalerite flake, with dissolution pits, associated with aggregates of spherical sphalerite grains (at right). Sample KRS12, mound springs at Wheal Ellen. Back-scattered electron image (SEM).

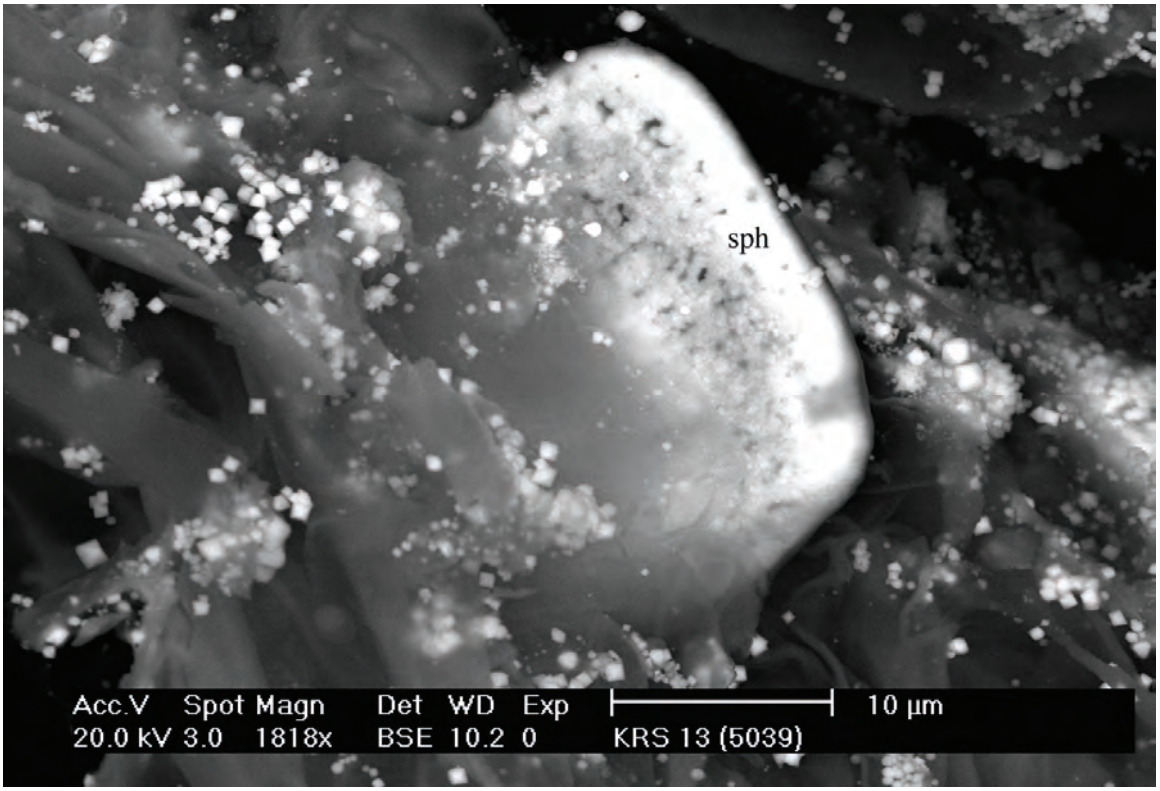

Figure 3.23. Rounded sphalerite (sph) grain embedded in organic matter and dusted by fine pyrite cubes. Sample KRS13, mound springs at Wheal Ellen. Back-scattered electron image (SEM).

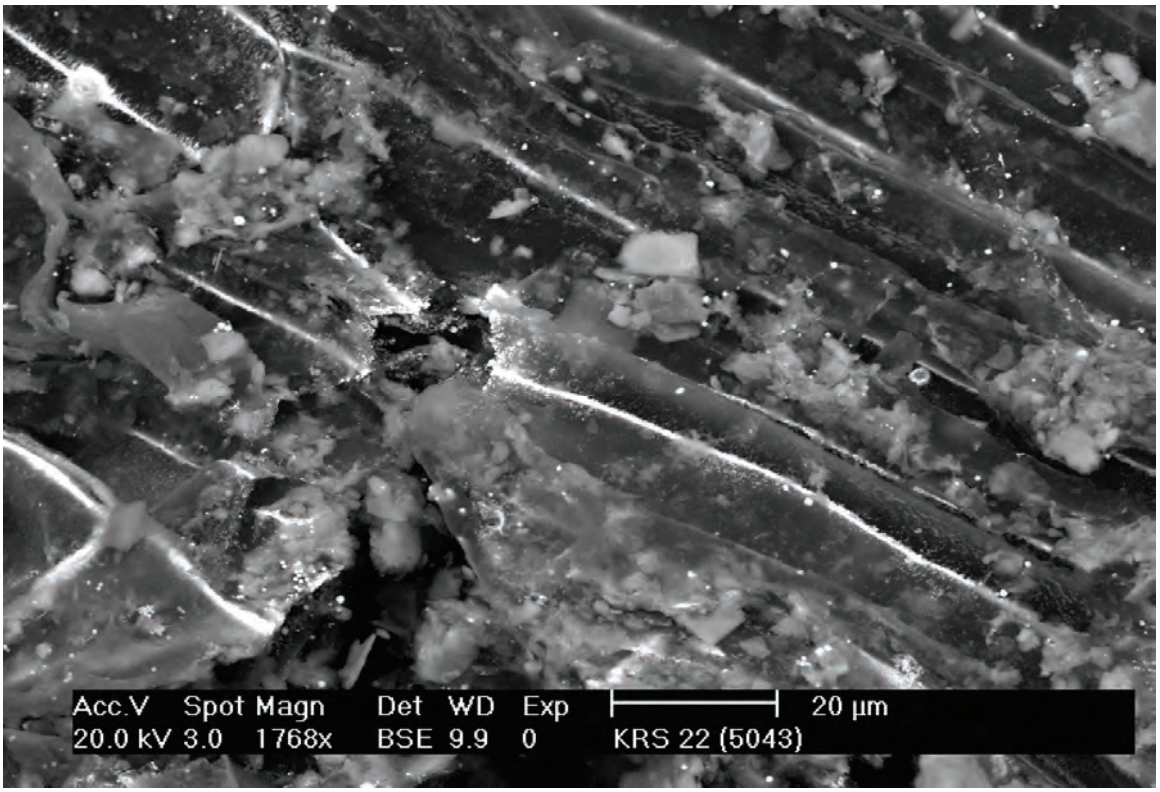

Figure 3.24. Very fine-grained linear aggregates of sphalerite, galena and pyrite precipitated between plant cell walls. Sample KRS22. Back-scattered electron image (SEM).

Galena

Galena is less common than sphalerite. It occurs in acid sulfate soils from the mound springs at Wheal Ellen, the wetland along Rodwell Creek to the south of Wheal Ellen, and from a seep to the north, and along strike from, the Mt Torrens prospect. It occurs as:

(i) intergrowths with sphalerite, coated by clays, or with clays and pyrite;
(ii) very fine-grained linear aggregates of sphalerite, pyrite and galena between plant cell walls (Figure 3.24);
(iii) globular aggregates <1 μm in diameter (Figure 3.25).

Chalcopyrite

Chalcopyrite is relatively rare and occurs in the wetland along Rodwell Creek to the south of Wheal Ellen, and in Dawesley Creek, near the old Paringa Cu-Au-Ag-Pb mine, south of Kanmantoo. It occurs as:

(i) fine-grained intergrowths with sphalerite and galena;
(ii) disseminated subhedral grains, associated with pyrite (Figure 3.26).

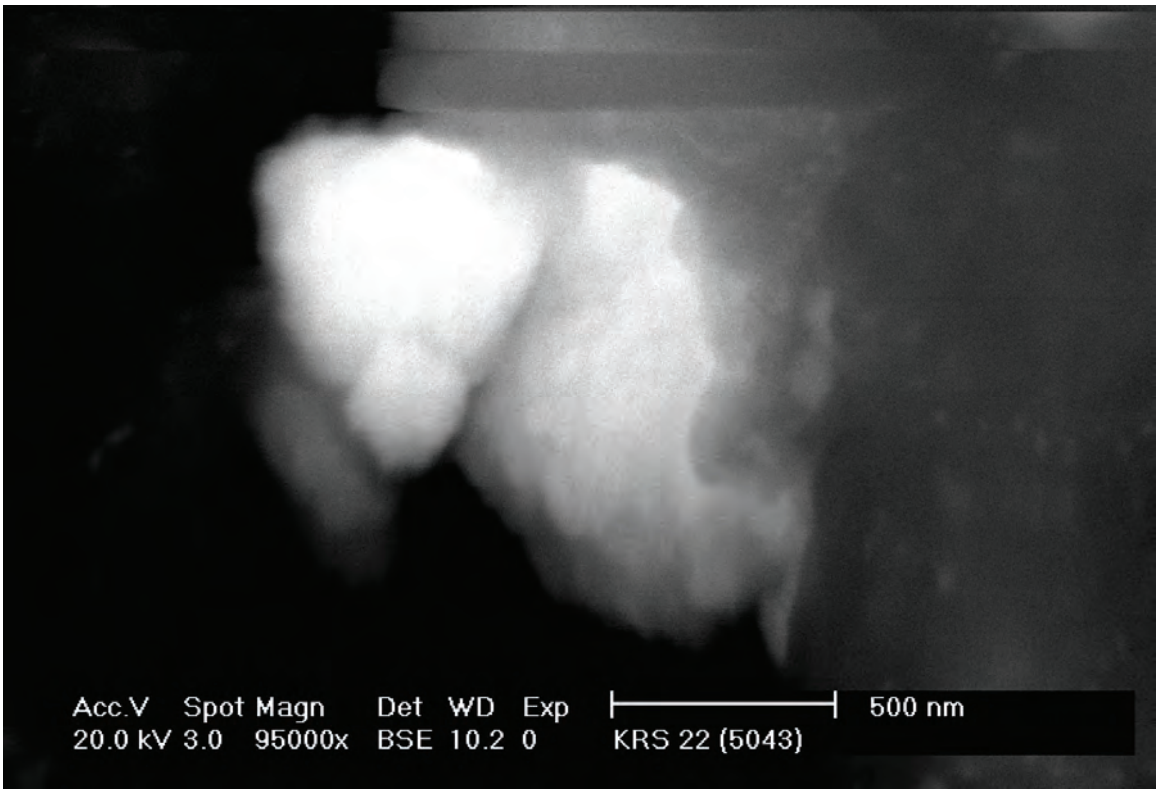

Figure 3.25. Aggregate of globular to botryoidal galena grains embedded in mica. Sample KRS22. Back-scattered electron image (SEM).

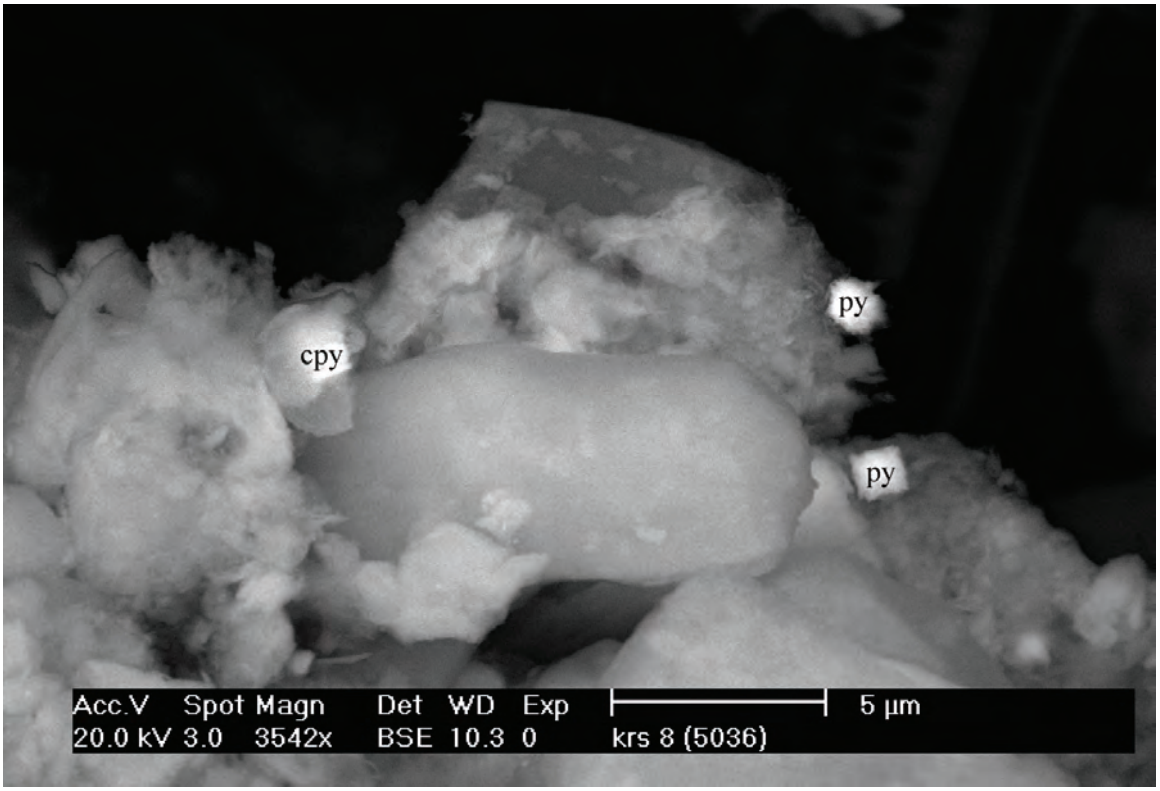

Figure 3.26. Disseminated subhedral to euhedral chalcopyrite (cpy) and pyrite (py) grains on quartz and kaolin. Sample KRS8. Back-scattered electron image (SEM).

3.2.2. Mn oxides

Manganese oxides were recorded from the springs at Wheal Ellen and from Dawesley Creek, near the old Paringa mine. Those from Wheal Ellen contain variable minor amounts of Zn, Co and I, whereas those from Dawesley Creek only contain Co. Manganese oxides occur as:

(i) botryoidal aggregates, encrusted by pyrite (Figure 3.16);
(ii) anhedral grains associated with organic matter (Figure 3.27);
(iii) intergrowths with Fe oxides (Figure 3.17).

3.2.3. Native gold

One grain of native gold (containing no detectable Ag) was found embedded in clays (Figure 3.28) from Dawesley Creek, near the old Paringa mine.

3.2.4. Barite

Barite was recorded from the springs at Wheal Ellen and from Glenalbyn. It occurs as:

(i) clusters of platy grains (Figure 3.29);
(ii) euhedral grains on clays;
(iii) anhedral grains with dissolution features (Figure 3.30).

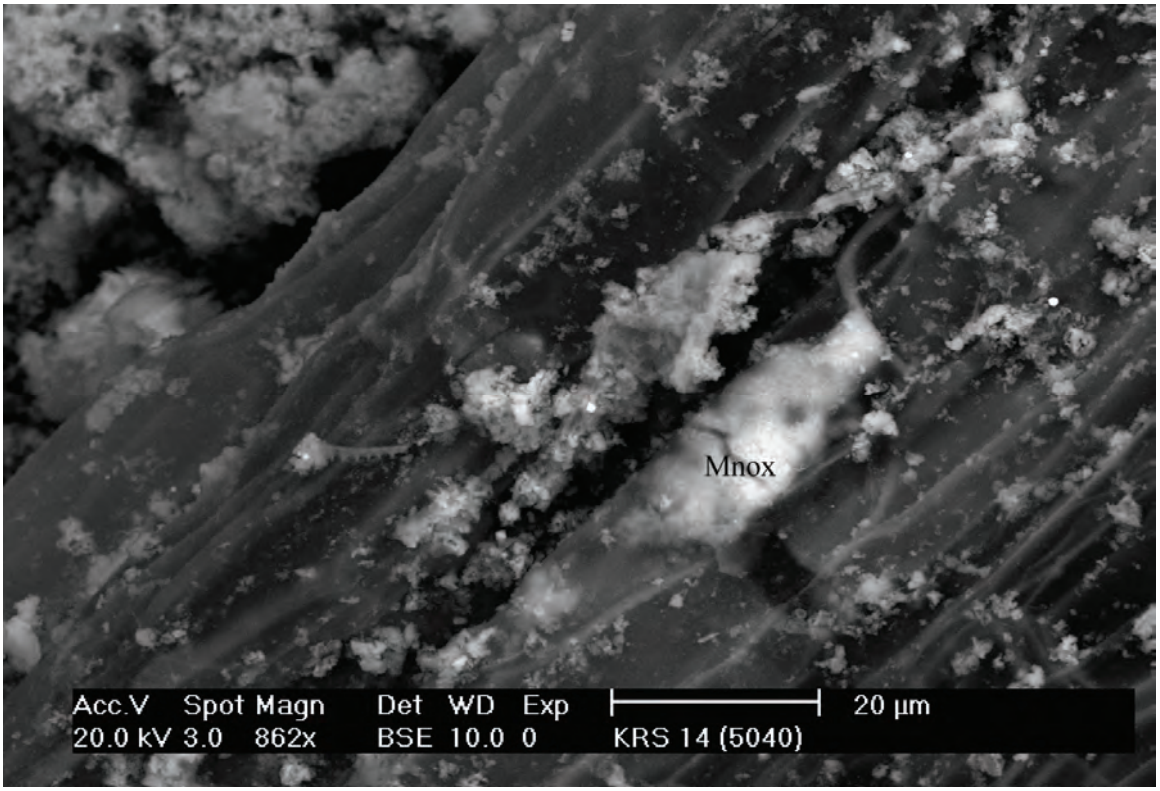

Figure 3.27. Iodine-bearing Mn oxide (Mnox) on organic matter and associated with minor disseminated pyrite. Sample KRS14, mound springs at Wheal Ellen. Back-scattered electron image (SEM).

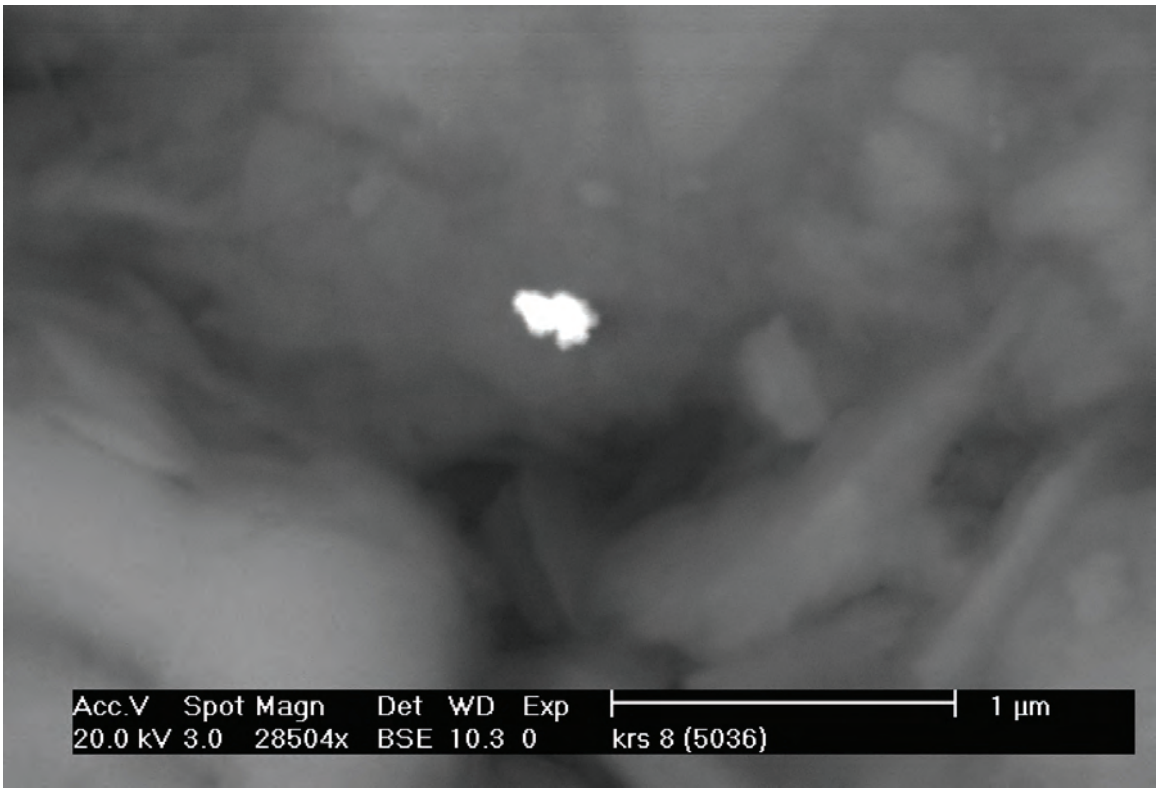

Figure 3.28. Anhedral grain of native gold embedded in kaolin. Sample KRS8. Back-scattered electron image (SEM).

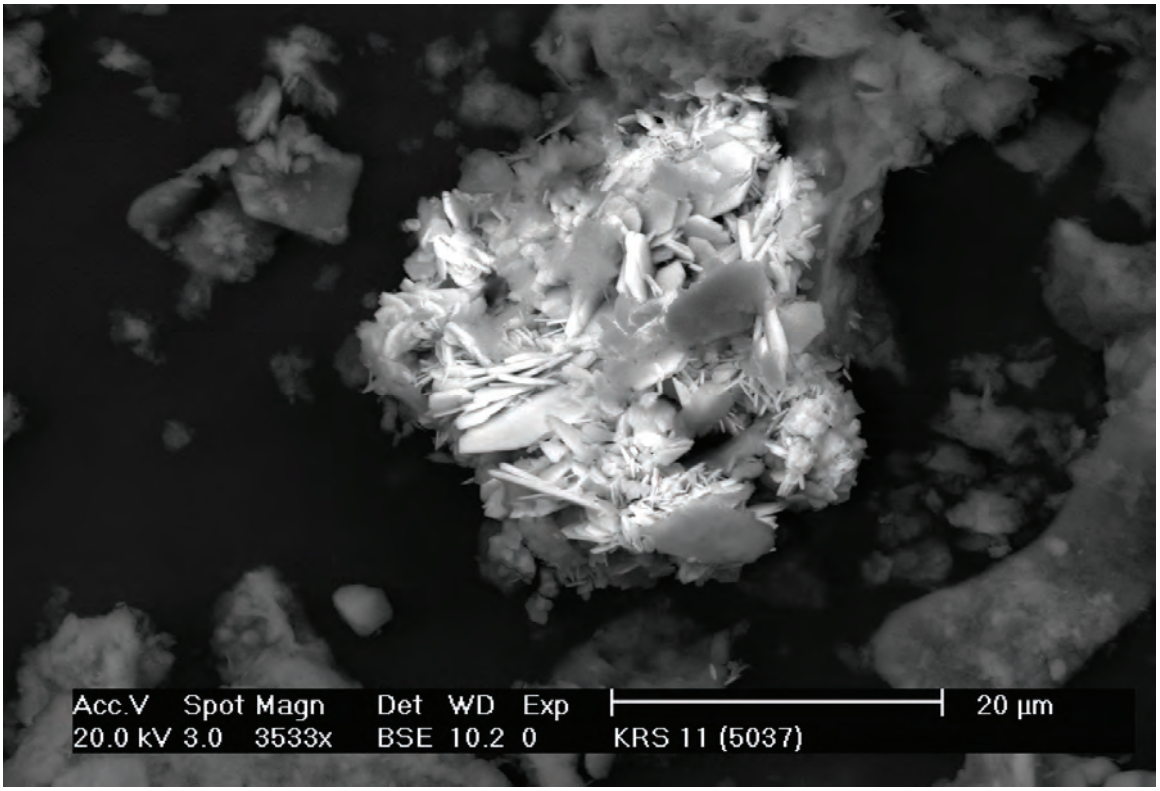

Figure 3.29. Aggregate of barite platelets associated with quartz and kaolin. Sample KRS11, Glenalbyn mine. Back-scattered electron image (SEM).

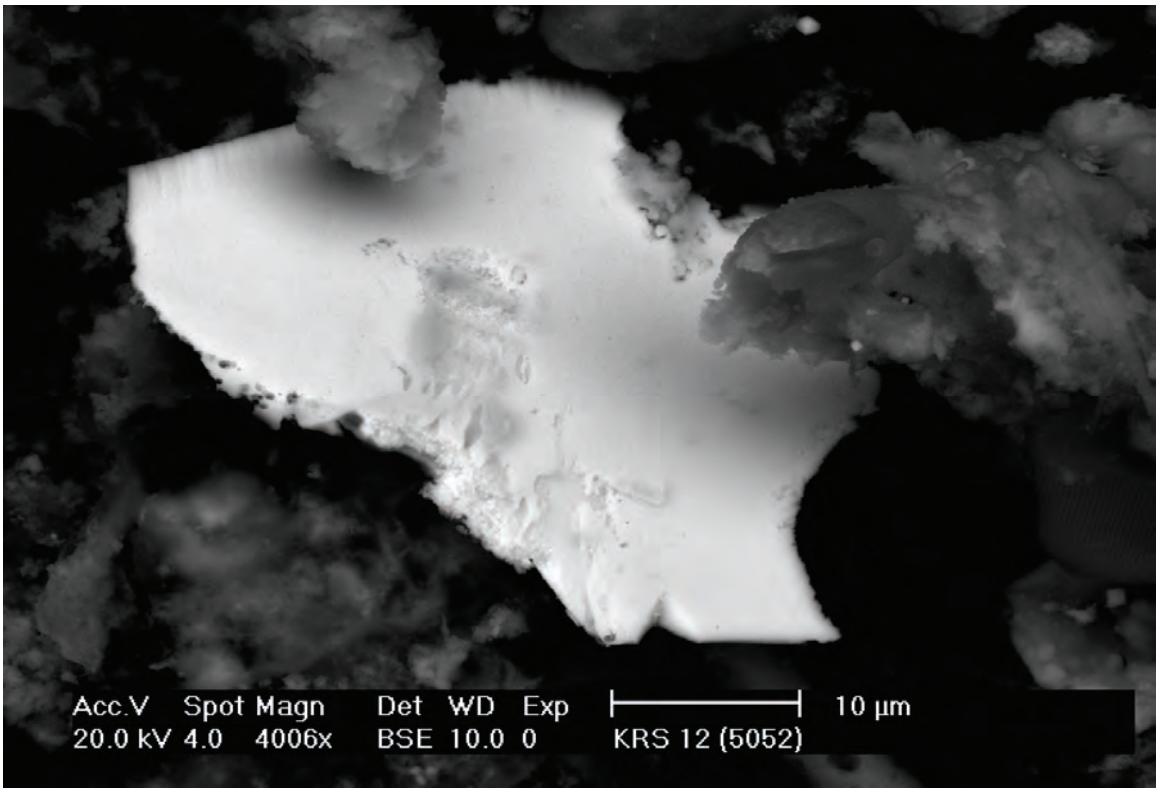

Figure 3.30. Anhedral barite platelet, associated with quartz and kaolin, with dissolution pits. Sample KRS12, mound springs at Wheal Ellen. Back-scattered electron image (SEM).

4. GEOCHEMISTRY

4.1 Ore zones in bedrock

Selected samples (Appendix 1c) of fresh or weathered mineralization from the some of the mines/prospects (Mount Torrens prospect, Bremer mine, Glenalbyn mine, Wheal Ellen, Wheal Margaret and the Monarto Cu prospect) in the district were analysed to obtain indications of the geochemical signatures of the various deposits. The results indicate that there are three broad element associations commensurate with the broad commodity-based mineralization types listed above (Cu±Au, Pb-Zn-Ag±Au, and Cu-As±Au):

Cu±Au: Cu-Au-Ag-Bi-Cd-Co-In±As±Sb±Te±Zn;

Pb-Zn-Ag±Au: Pb-Zn-Ag-Bi-Cd-Co-Hg-In-Mn-Mo-Sb-Tl±As±Au±Cu;

Cu-As±Au: Cu-As-Ag-Mo-Sb-Te±Au±Bi±Tl.

4.2 Regional geochemistry of acid sulfate soil materials

4.2.1 Ore-associated elements

The regional distribution patterns are shown in Appendix 3a and summarized in Table 1. The following trends were noted in the vicinity of known mines and prospects:

(i) Wheal Ellen (Cu±Au): anomalous Ag, Au, Bi, Cd, Co, Cu, Hg, In, Mo, Ni, Pb, Sb, Se, Tl and Zn (samples KRS12-14; KRS16-17; KRS20-21);
(ii) Kanmantoo area (Cu±Au): anomalous Au, Bi, Co, Cu, Ni, Se and Tl (samples KRS8, KRS45);
(iii) Mount Torrens prospect (Pb-Zn-Ag±Au): anomalous As, Bi, Hg, Ni, Pb and Tl (samples MT050, MT053-054; MT056-057);
(iv) Monarto Cu prospect (?Cu-As±Au): anomalous Cd and Tl (sample KRS101);
(v) Glenalbyn (Cu-As±Au): anomalous Cu and Mo (sample KRS11).

The following anomalies are not related to known occurrences of mineralization (e.g., Figures 4.1, 4.2, 4.3 and 4.4, and Table 1):

(i) north of Brukunga (Pb-Zn-Ag±Au): anomalous Cd and Zn (sample KRS123);
(ii) Guthries (Pb-Zn-Ag±Au): anomalous Ag, As and Tl (samples KRS146-147);
(iii) north of Wheal Ellen (Pb-Zn-Ag±Au): anomalous As and Tl (samples KRS118-119);
(iv) south-east Harrogate (Pb-Zn-Ag±Au): anomalous Zn (sample KRS143);
(v) Bottroffs Hill (Cu-As±Au): anomalous Cu (sample KRS79);
(vi) Collins Road (Cu-As±Au): anomalous Au (sample KRS152);
(vii) south-east Mount Barker (Pb-Zn-Ag±Au): anomalous Zn (sample KRS115);
(viii) east of Wheal Ellen (Cu±Au): anomalous Ag, Au, Bi, Cd, Hg, In, Pb, Sb, Se and Zn (sample KRS22).

Trace element concentrations are independent of Fe, Mn or S contents of the samples. Estimated background and threshold limits for selected elements are shown in Table 2.

Most of the anomalies overlie Tapanappa Formation lithologies, consistent with this unit being the principal host to mineralization in the Kanmantoo (Belperio et al., 1998; Toteff, 1999). Three anomalies (Mount Torrens, north of Wheal Ellen, and north of Brukunga) are related to the Talisker Calc-siltstone and may belong to the same class of mineralization (Pb-Zn-Ag±Au). The anomalies at Wheal Ellen and KRS22 are related to garnet- and Mn-rich alteration zones (metamorphosed

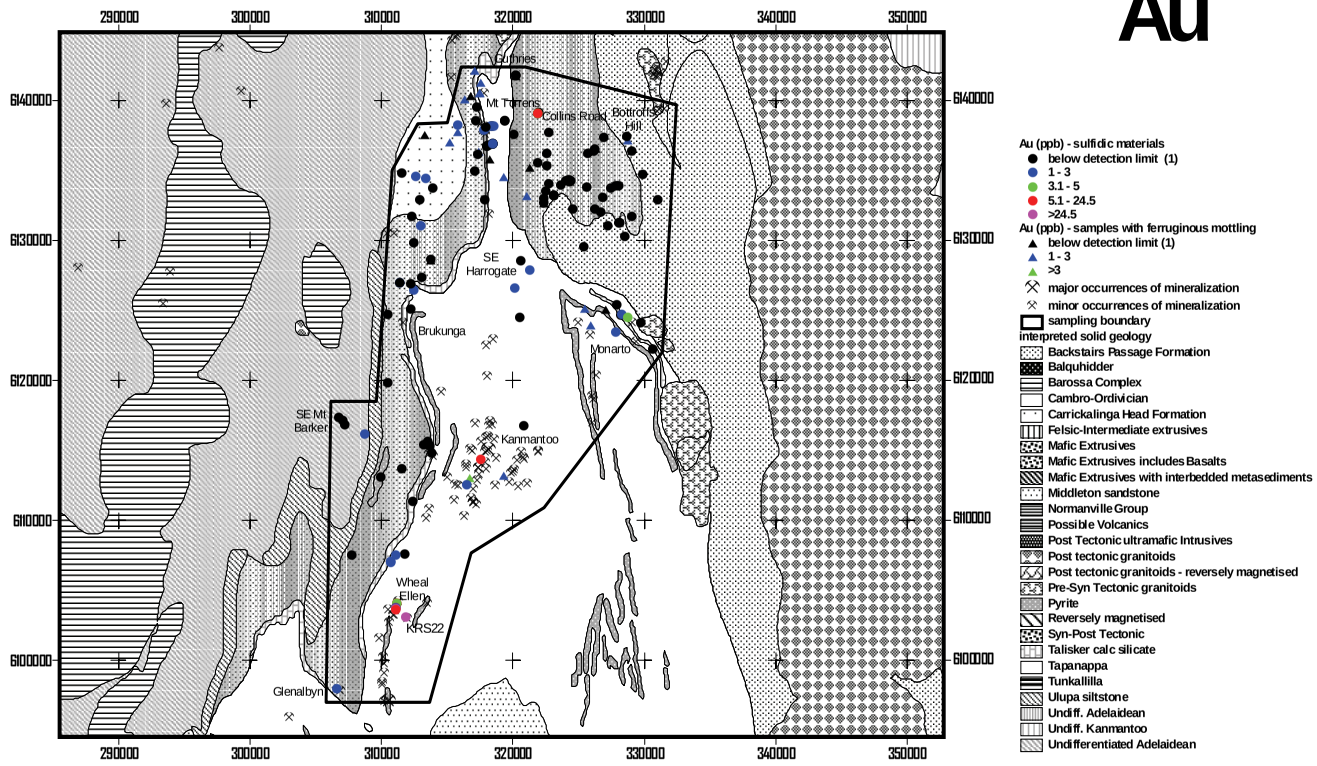

Figure 4.1. Distribution of Au (ppb) in acid sulfate soils showing locations of the anomalies in relation to distribution of geological units. The geological map is taken from the PIRSA Kanmantoo GIS package.

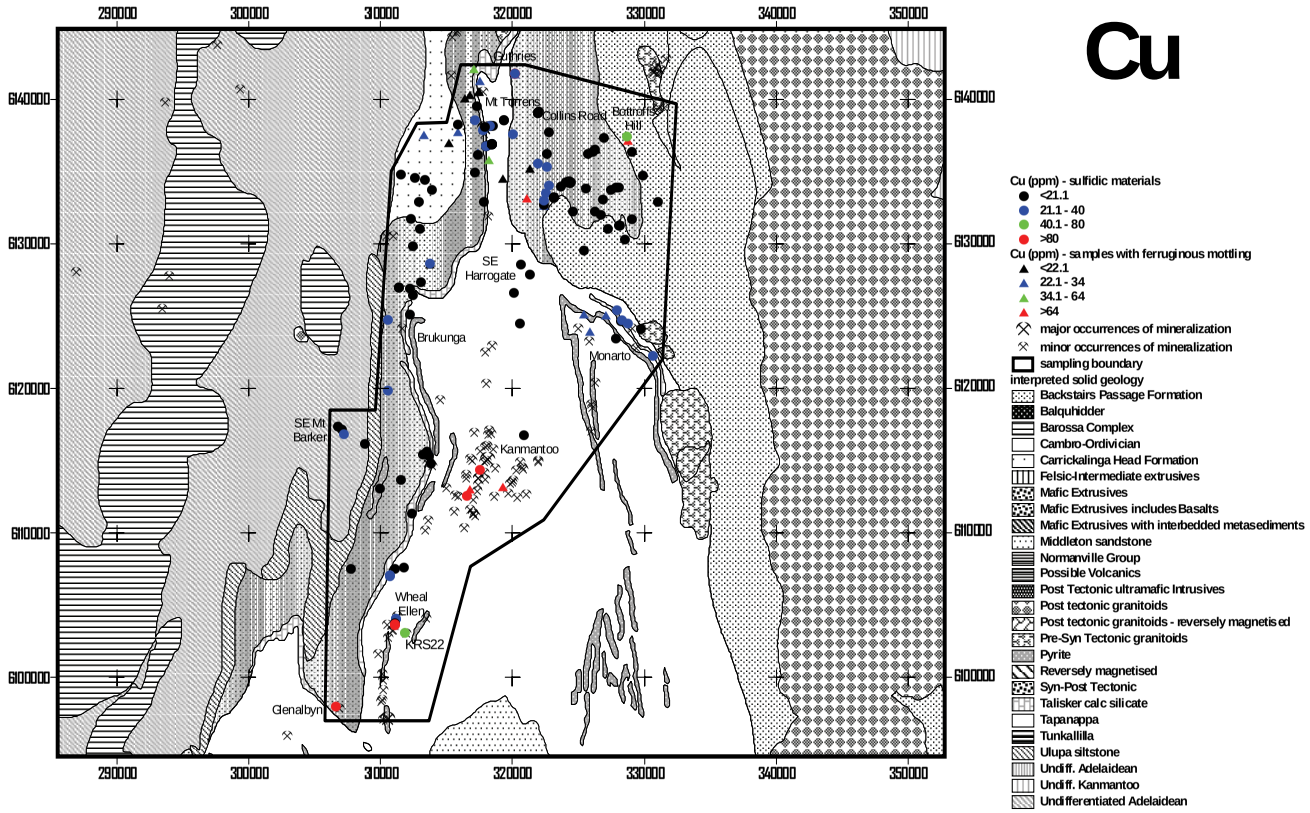

Figure 4.2. Distribution of Cu (ppm) in acid sulfate soils showing locations of the anomalies in relation to distribution of geological units. The geological map is taken from the PIRSA Kanmantoo GIS package.

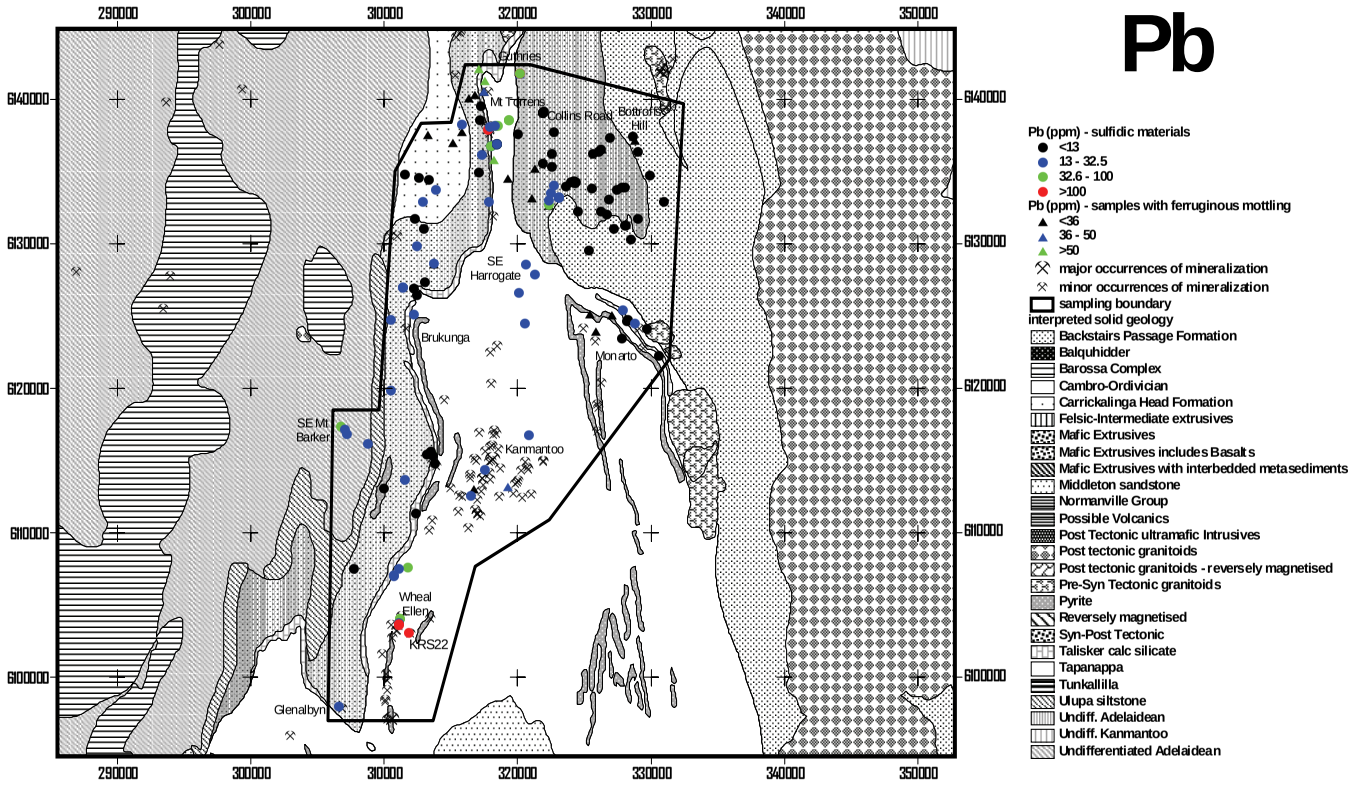

Figure 4.3. Distribution of Pb (ppm) in acid sulfate soils showing locations of the anomalies in relation to distribution of geological units. The geological map is taken from the PIRSA Kanmantoo GIS package.

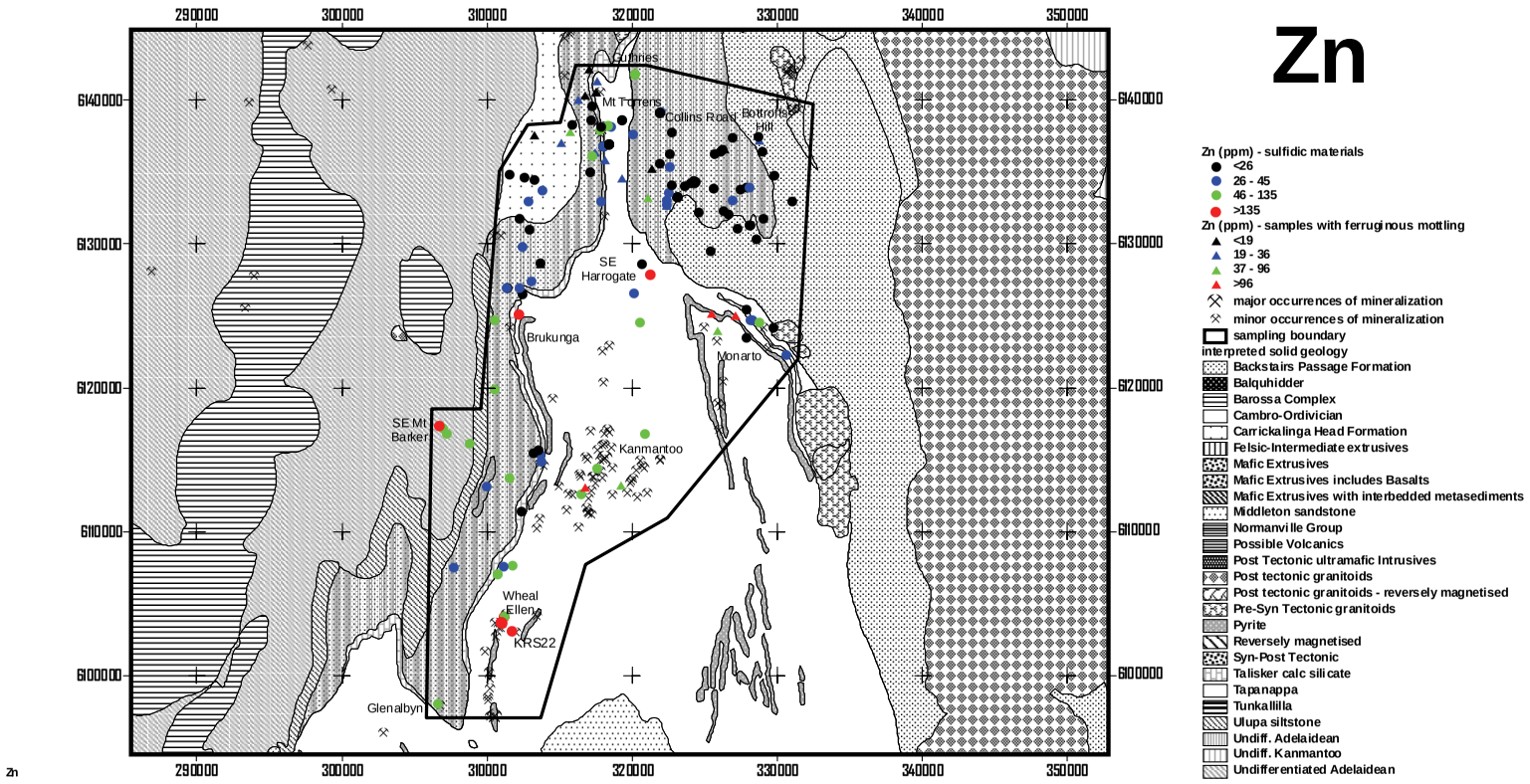

Figure 4.4. Distribution of Zn (ppm) in acid sulfate soils showing locations of the anomalies in relation to distribution of geological units. The geological map is taken from the PIRSA Kanmantoo GIS package.

Table 1. List of geochemical anomalies showing maximum concentrations of anomalous elements. All values in ppm, except Au (ppb).

Anomaly	Ag	As	Au	Bi	Cd	Co	Cu	Hg	In	Mo	Ni	Pb	Sb	Se	Tl	Zn
Wheal Ellen	2.3		36	5.5	1.8	3150	115	0.1	0.5	25.5	140	1050	2.5	1.5	0.9	15800
Kanmantoo area			19	11			650				45			2.5	1.1	
Mount Torrens		55		1				0.05			44	200			0.9	
Monarto					1										0.8	
Glenalbyn							750			6.5						
north of Brukunga					0.8											310
Guthries	0.4	17													1	
north of Wheal Ellen		24													0.8	
south-east Harrogate																600
Bottroffs Hill							120									
Collins Road			24.5													
south-east Mount Barker												56				190
KRS22	7.5		45	2	14			0.05	0.3		9	2850	8	2		2600

exhalites), locally with pyrite-pyrrhotite bodies (Toteff, 1999), rather than to the Nairne Pyrite Member. Sulfidic materials overlying the Backstairs Passage Formation are rarely anomalous (except

Table 2. Estimated backgrounds and thresholds (in ppm, except where stated) for selected elements in sulfidic materials.

Element	Background	Threshold
Ag	0.2	0.4
As	10	16
Au (ppb)	3	5.1
Bi	0.3	0.6
Cd	0.3	0.6
Co	8.5	100
Cu	40	80
In	<0.05	0.15
Mo	2	5.5
Ni	16	32
Pb	32.5	100
Sb	<0.5	1.6
Se	<0.5	1.1
Tl	0.4	0.7
Zn	25	135

at the Collins Road anomaly (Au, Figure 4.1) and at Bottroffs Hill (Cu; Figure 4.2).

The anomaly at KRS22 is the most significant anomaly that cannot be related to known mineralization, in terms of concentration levels (Table 1) and the number of anomalous elements (10). The other anomalies are difficult to rank, without more detailed local geological investigations and/or analysis of Pb and S isotopes, to determine their relationships to mineralization.

4.2.2 Lithophile elements

There is a distinct contrast in the geochemical relationship between Na and K on either side of the Bremer Fault (Figures 4.5 and 4.6), which probably reflects geochemical differences in the detrital fraction of the sample. Samples to the east of the fault are characterized by greater concentrations of Na and a negative correlation between Na and K, except for a small subgroup of samples with both relatively low Na and K contents. To the west of the fault, samples exhibit a positive correlation between Na and K. Other elements (Ba, Rb, Sr and Tl) also exhibit geochemical differences similar to K (Appendix 3b), with positive correlation factors with Na west of the fault, but negative east of it. In contrast, Al has positive correlation factors with Na on both sides of the fault, despite distinct groupings on a Na-Al plot (Appendix 3b). This could suggest that Na occurs in an Al-bearing phase, such as plagioclase, with more calcic compositions to the west of the fault, and more Na-rich compositions to the east.

These differences may reflect regional addition of Na, or loss of K, east of the fault, rather than addition of K west of it. These differences in alkali chemistry in the Kanmantoo Group have not been previously documented and the reasons for this variation are not clear, but may relate to regional fluid flow related to mineralization in the west, to differences in regional metamorphism between east and west, or granitoid intrusion and regional metasomatism in the east.

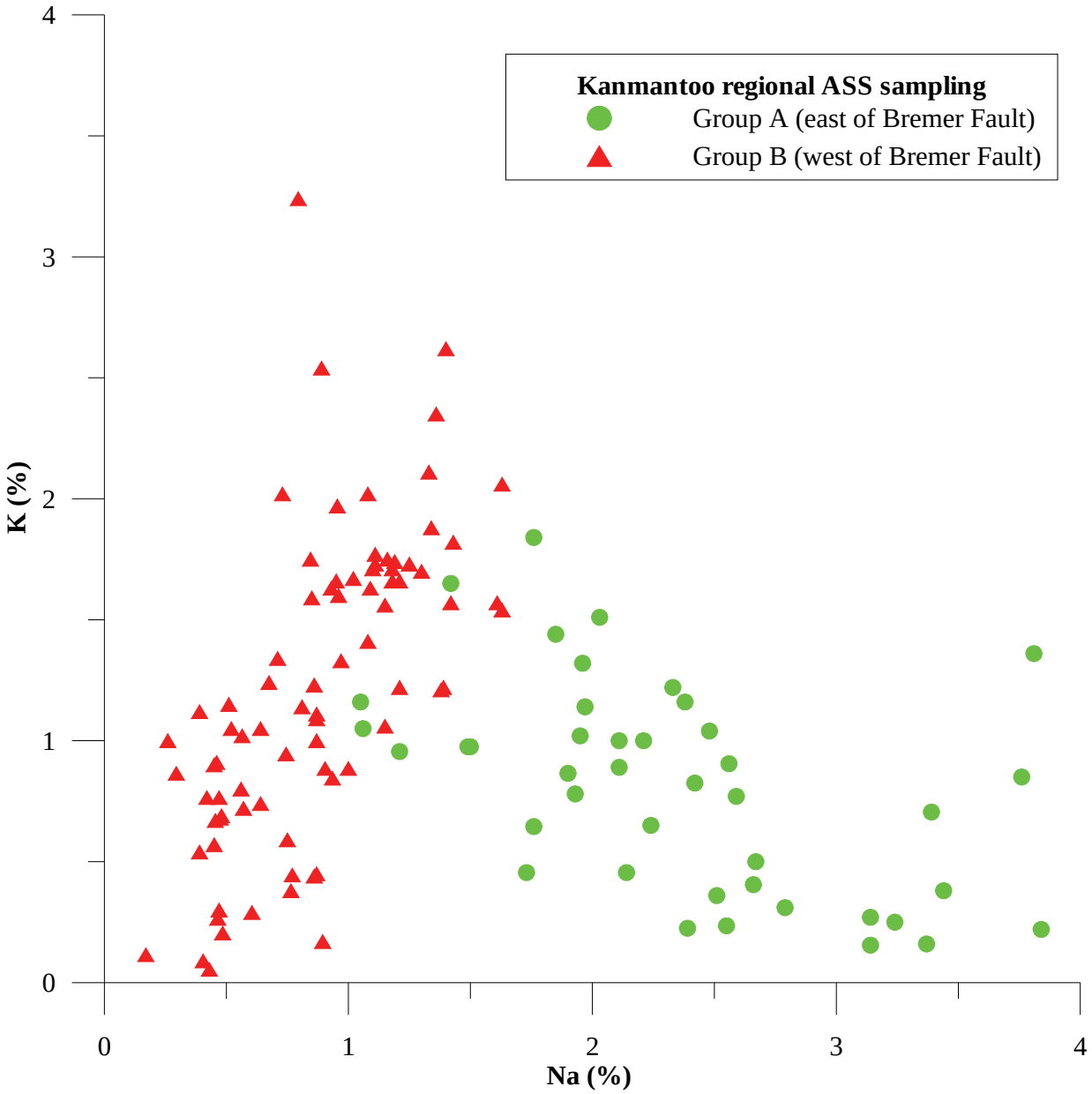

Figure 4.5. The distribution of Na and K in sulfidic material from acid sulfate-like soils on either side of the Bremer Fault. Group A samples occur on the eastern side of the fault and exhibit a distinct negative correlation between Na and K. Group B samples occur on the west side of the fault and exhibit positive correlation between Na and K. Samples (red triangles) close to the origin of the graph plot to the east of the Bremer Fault in Figure 4.3.

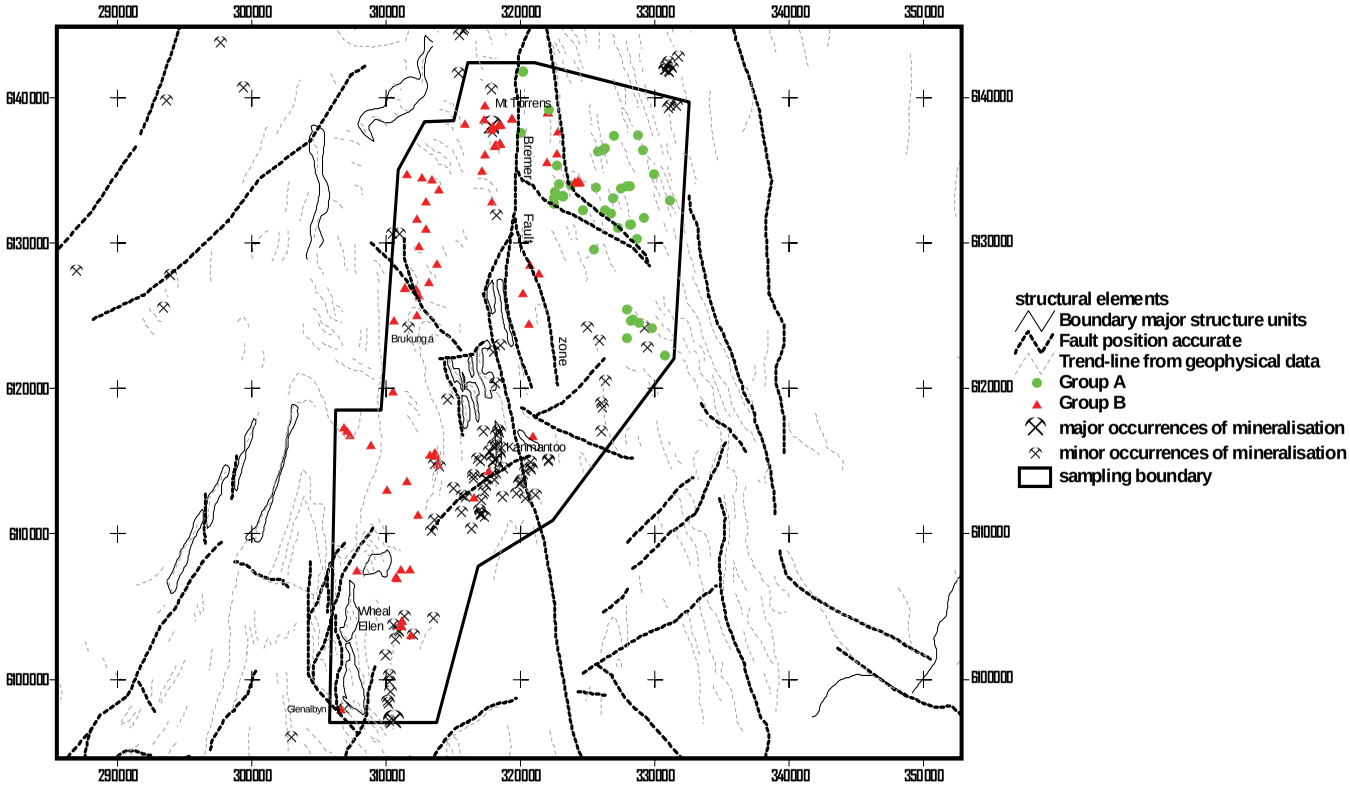

Figure 4.6. The distribution of the two groups of sulfidic material from acid sulfate-like soils in relation to the Bremer Fault.

5. HYDROGEOCHEMISTRY

The surface waters at acid sulfate soil sample sites vary considerably in composition, from non-saline to extremely saline and from weakly acidic to alkaline (Appendix 5; Figures 5.1 and 5.2). In general terms, the relatively low-salinity waters occur in the higher-rainfall areas in the west and the most saline waters generally occur in the lower-rainfall areas in the east. There is, however, a saline wedge in the north and north-east. There is no obvious relationship between electrical conductivity (EC) and sample type (Figure 2.2). It would appear that factors other than total rainfall are responsible for the local variations in EC: these could include evaporation within restricted pools enhancing salinity, precipitation of salts within restricted pools, or subsurface contributions of groundwater to surface waters.

Most of the slightly acidic to near-neutral surface waters occur in the higher rainfall areas in the north-west, there are also significant local variations (Figure 5.2). Some of the sites with lower pH in the east are from springs and seeps, but several are from creeks. It is possible that some of these lower pH values have resulted from the incipient oxidation of acid sulfate soils.

Some major ions (Na^+, Mg^{2+}, K^+, Sr^{2+}) match the seawater trend reasonably well (Figure 5.3), whereas others (Ca^{2+}, SO_4^{2-}, BO_3^{3-}) are relatively poorly correlated with it (Figure 5.4), implying some degree of supersaturation. The spatial distribution of most elements closely follows that of EC: where EC values are relatively large, concentrations of Na^+, K^+, Mg^{2+}, Ca^{2+}, Sr^{2+} and SO_4^{2-} tend to be greater (Figure 5.5). In terms of sample types, samples from wetlands have the greatest concentration levels of Ca^{2+}, Na^+, Mg^{2+}, K^+, Sr^{2+}, SO_4^{2-} and BO_3^{3-}, the largest EC values, and pH values trending to <5 (Figure 5.6; Appendix 7).

Some neutral to weakly alkaline samples contain detectable Al, Fe, Mn and excessive Si (David Gray, pers.comm., 2002), indicating that they contain some suspended material (clays, ferrihydrite, quartz). Consequently, the results for these elements need to be treated with caution. Zinc is present in some samples, but some of these are weakly alkaline and may also indicate some presence of suspended clays and ferrihydrite, which could be the source of Zn. However, the sample from Wheal Ellen contains 0.345 ppm Zn (in near-neutral solution; Appendix 6), which could indicate surface water may be a valid sampling medium, if proper sampling protocols are followed and pH is monitored.

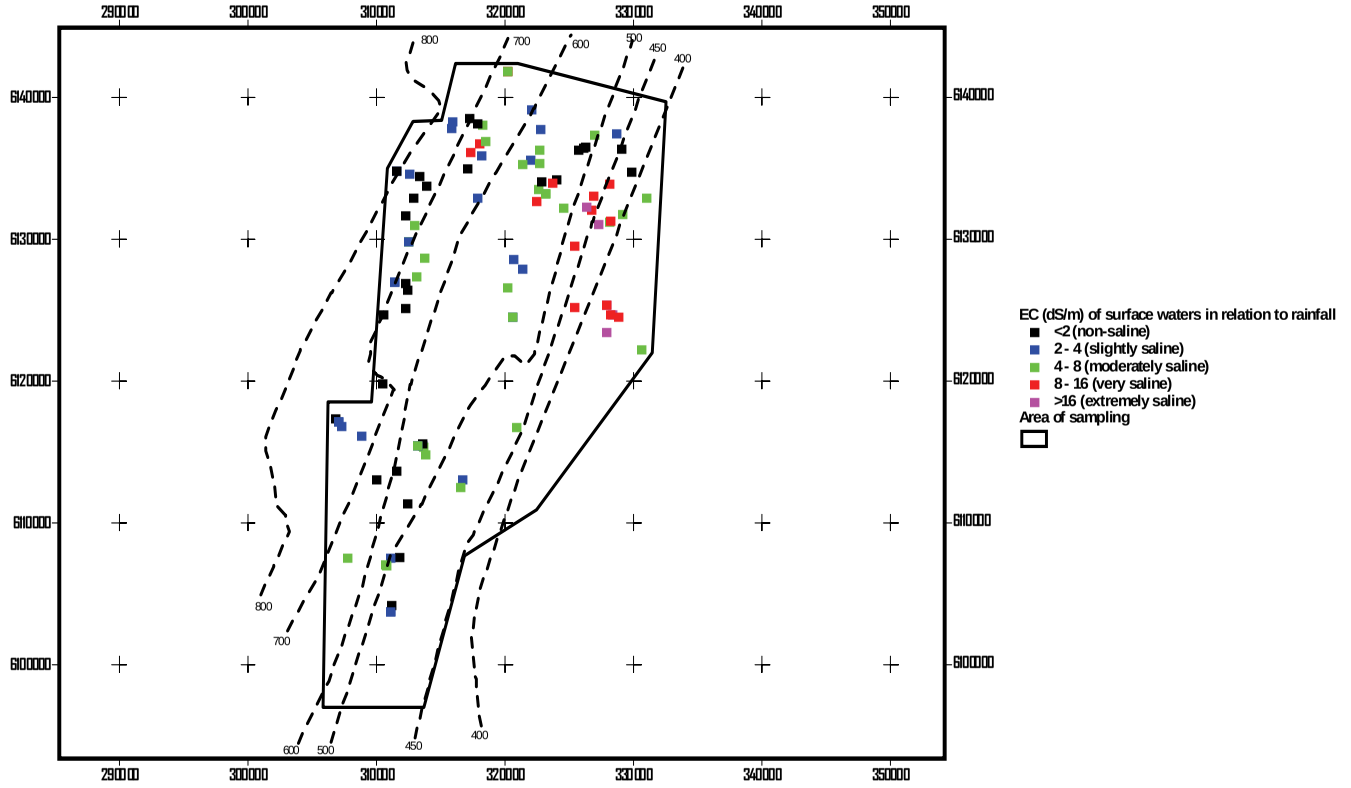

Figure 5.1. The electrical conductivity (EC) of surface waters in relation to average rainfall isohyets (mm).

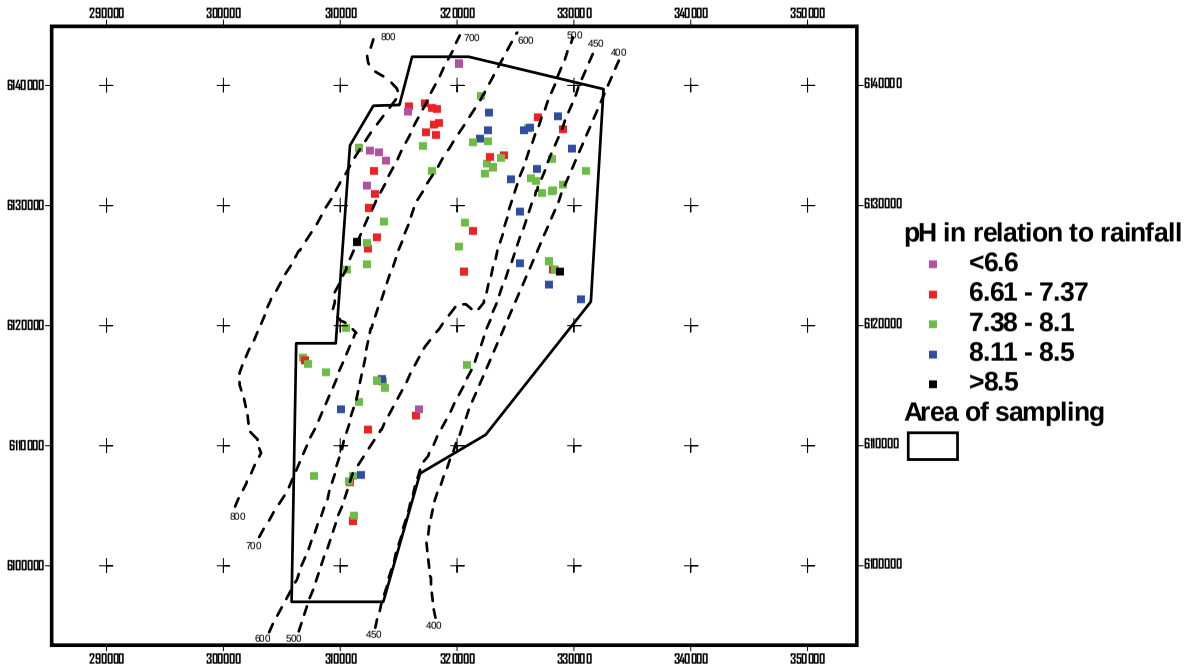

Figure 5.2. Values of pH in relation to average rainfall isohyets (mm).

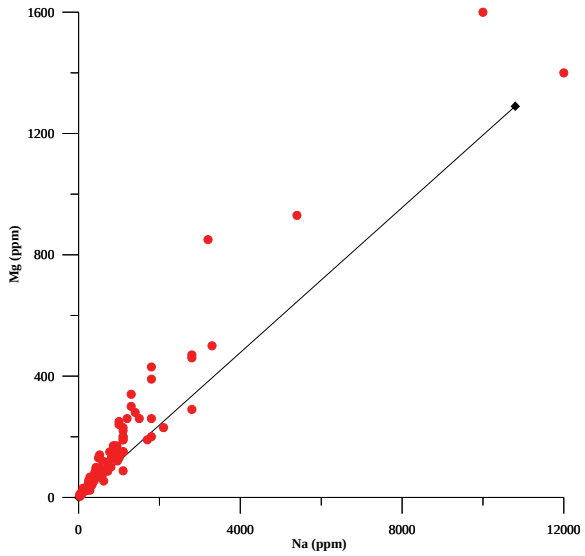

Figure 5.3. A plot of Na versus Mg showing the correlation of Mg with the seawater trend (black line).

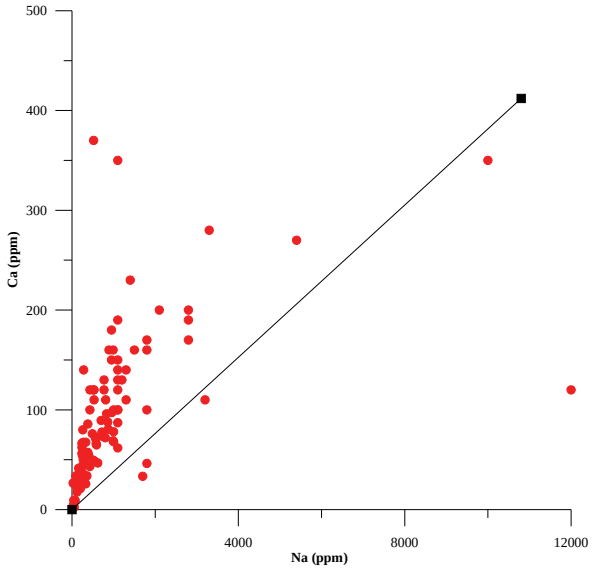

Figure 5.4. A plot of Na versus Ca showing the poor correlation of Ca with the seawater trend (black line).

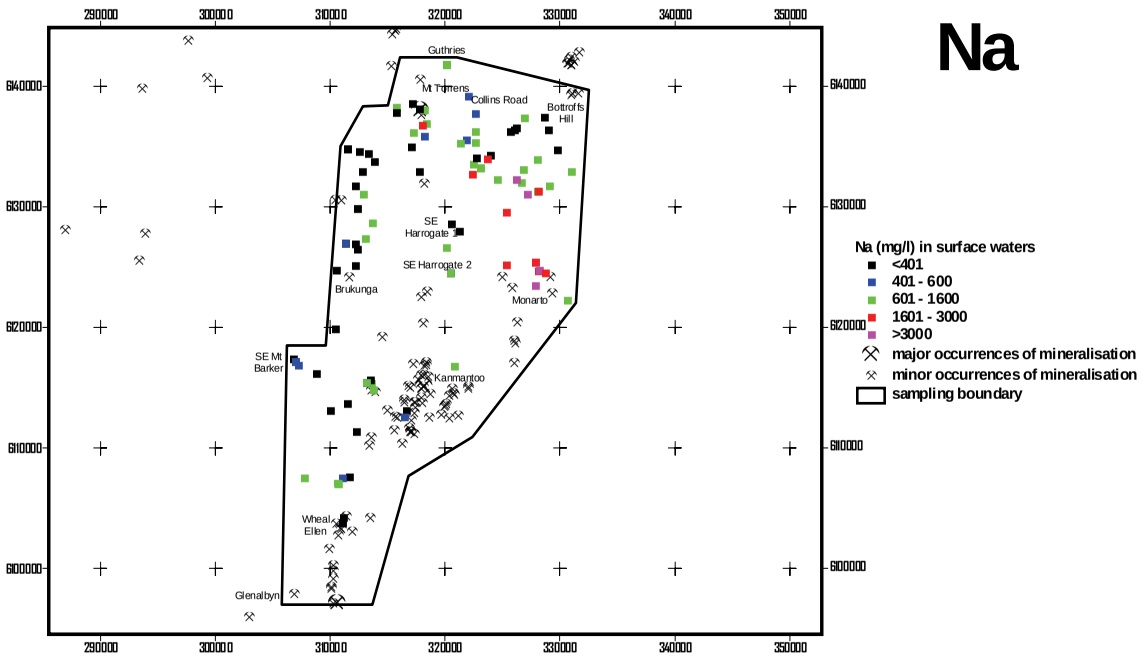

Figure 5.5. The spatial distribution of Na (ppm, or mg/l) in surface waters. Samples with greater Na concentrations correlate closely with those samples with higher values of electrical conductivity (EC).

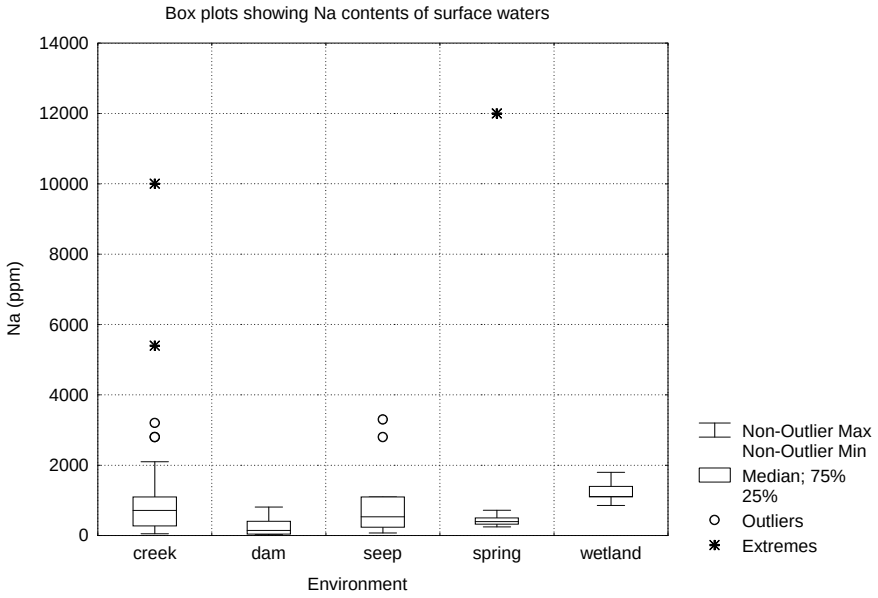

Figure 5.6. Box plots showing the distribution of Na in surface waters from creeks, dams, seeps, springs and wetlands. The data suggest that waters from wetlands are consistently more saline than those from other environments.

6. CONCLUSIONS

(1) Results indicate that acid sulfate soil materials in seeps, springs, wetlands and creeks represent a new sampling medium. This investigation has shown that not only are geochemical anomalies related to known mineralization, but also that new generations of sulfides (pyrite, sphalerite, galena, chalcopyrite) and native gold have precipitated in environments close to these mineralized zones. A soil-landscape model illustrating geochemical dispersion into acid sulfate materials from mineralized zones into seeps, springs and wetlands is shown in Figure 6.1. Lateral groundwater and through flow transport metals of interest to reduced seepages, where secondary sulfides are precipitated. In some instances, there is clear evidence (from textural data) for biomineralization being involved in the precipitation of secondary sulfides. These findings clearly corroborate the findings of the orientation survey at the Mount Torrens prospect (Skwarnecki et al., 2002a).

(2) Geochemical anomalies in acid sulfate soils do not provide drilling targets in themselves. On a regional scale, they are comparable to stream-sediment sampling, but are a more robust sampling medium, in that acid sulfate soils provide a more direct geochemical and mineralogical manifestation of mineralization. Additionally, geochemical anomalies in acid sulfate soils can detect blind zones of mineralization, whereas stream-sediment sampling can only detect mineralization that is, or was, exposed in outcrop and eroded into drainages.

(3) There is a regional contrast in Na and K geochemistry across the Bremer Fault zone. This indicates the presence of fundamentally different geochemical provinces.

(4) The spatial distribution of most elements in groundwater closely follows that of electrical conductivity (EC), which delineates a saline wedge in the east, where sulfidic materials in creeks are relatively common.

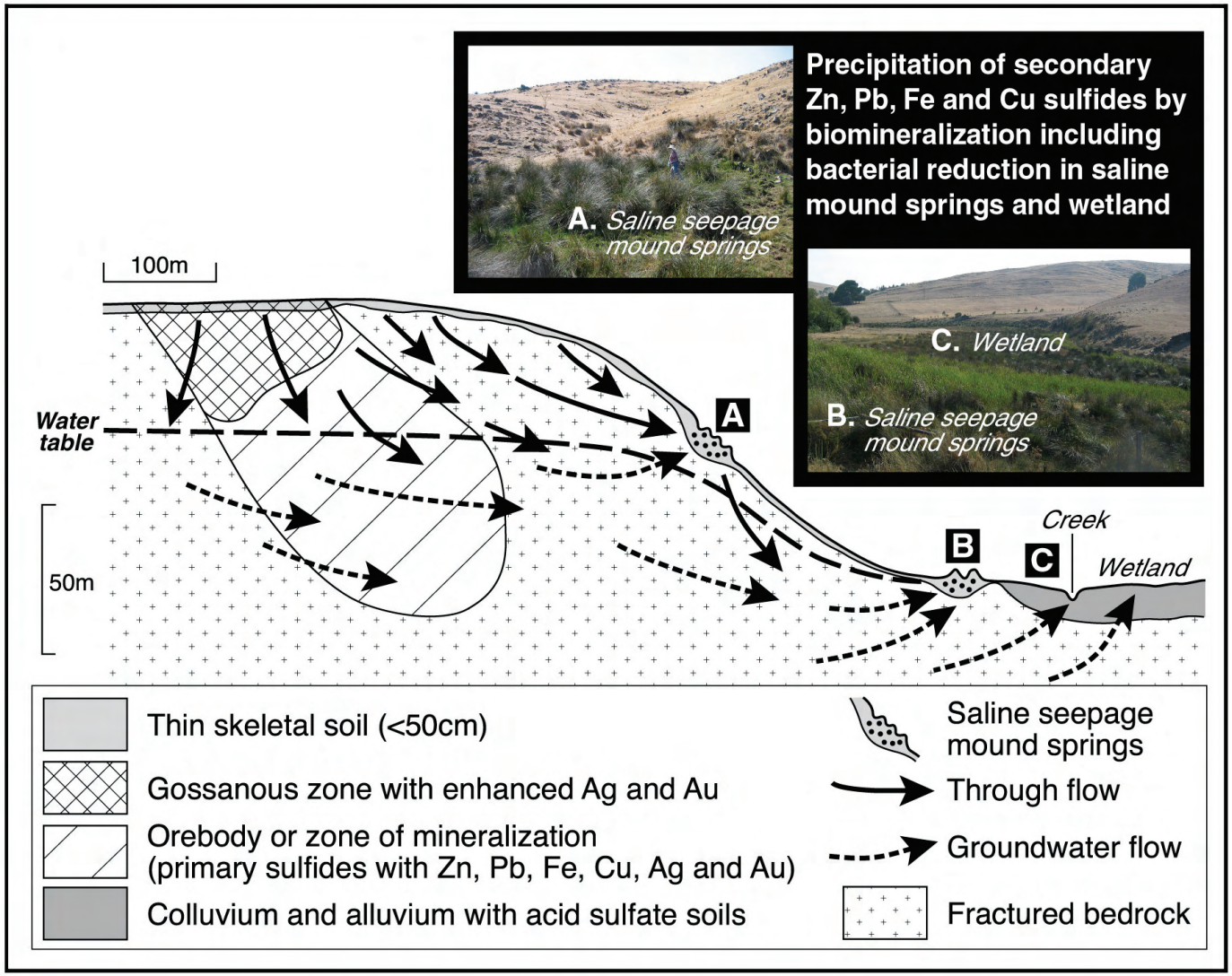

Figure 6.1. Model for geochemical dispersion from mineralized zones into acid sulfate materials in seeps, springs and wetlands, Mount Lofty Ranges.

(5) Future investigations should focus on:

(i) following up anomalies not attributable to known mineralization, especially KRS22;
(ii) mapping the distribution of acid sulfate soils and characterising their mineralogy and composition over a wider region in the Mount Lofty Ranges and other parts of Australia;
(iii) regional sampling of seeps, constrained by catchments and areas of known mineralization, together with background areas with no known mineralization, to provide further case studies and a more robust evaluation of the technique;
(iv) isotopic (Pb, S) and hydrogeochemical studies to better constrain the processes of acid sulfate soil formation and to provide tracers of the mineralization, to follow-up the preliminary investigations of Giblin et al. (1994);
(v) further characterization of the highly reactive Fe monosulfide-bearing materials (monosulfide black oozes);
(vi) evaluation of coastal acid sulfate soils as a potential sampling medium;
(vii) detailed geochemical studies on either side of the Bremer Fault zone, to determine the reasons for the geochemical disparities on either side of the fault.

Sulfidic materials from acid sulfate soils can be sampled at both regional and local scales to yield Au and base metal anomalies and indications of mineralization. However, detailed geological mapping and soil, deep regolith and rock-chip sampling would still be required to pinpoint the source of the anomalies, since dispersion may extend for several hundred metres from mineralization (as at the Mount Torrens prospect (Skwarnecki et al., 2002a) or at Wheal Ellen (this study)). Where mineralization is blind, drilling to residual regolith or geophysical techniques in combination with other tools (such as lithogeochemistry, structural analysis, or mapping of alteration zones) will be required.

7. ACKNOWLEDGEMENTS

This research could not have been carried out without assistance from the following individuals and organizations:

Charles Butt – for his strong support of the project from its inception;
Mark Thomas, Richard Merry, Andrew Baker – sampling in the field;
Sean Forrester – assistance with sample preparation;
Greg Rinder – scanning diagrams and assistance with production of diagrams;
Stuart McClure – for assistance with the SEM and electron microprobe;
Mark Raven – for XRD patterns;
Andy Burtt (PIRSA) – for providing the sample of Wheal Ellen mineralization;
CRC LEME and CSIRO Exploration & Mining (through the Glass Earth project) - for providing financial assistance;
Keith Scott, Graham F. Taylor and Charles Butt – for their review of the manuscript and suggestions for improvement.

8. REFERENCES

Anon. (1924) The Preamimma arsenic-copper mine. Mining Rev., Dept Mines South Aust., 41, p.69-77.

Askins, P.W. (1968) Geochemical exploration around the Aclare mine and mineral deposits of the surrounding region. B.Sc. (Hons) thesis (unpubl.), University of Adelaide.

Belperio, A.P., Preiss, W.V., Fairclough, M.C., Gatehouse, C.G., Gum, J., Hough, J. & Burtt, A. (1998) Tectonic and metallogenic framework of the Cambrian Stansbury Basin – Kanmantoo Trough, South Australia. AGSO Journal of Australian Geology & Geophysics 17, no.3, p.183-200.

Both, R.A. (1990) Kanmantoo Trough – geology and mineral deposits. In: F.E. Hughes (ed.) – Geology of the mineral deposits of Australia and Papua New Guinea. Australasian Institute of Mining & Metallurgy, Monograph 14, p.1195-1203.

Brown, H.Y.L. (1908) Record of the mines of South Australia, 4th edition.

Bush, R.T. & Sullivan, L.A. (1997) Morphology and behaviour of greigite from a Holocene sediment in Eastern Australia. Australian Journal of Soil Research 35, p.853-861.

Butt CRM and Nichol I. (1979) The identification of various types of geochemical stream sediment anomalies in Northern Island. Journal of Geochemcial Exploration 11: 13 – 32.

Fitzpatrick, R.W., Naidu, R. & Self, P.G. (1992) Iron deposits and microorganisms in saline sulfidic soils with altered soil water regimes in South Australia. Catena Supplement 21, 263-286.

Fitzpatrick, R.W., E. Fritsch and P.G. Self (1996). Interpretation of soil features produced by ancient and modern processes in degraded landscapes: V Development of saline sulfidic features in non-tidal seepage areas. Geoderma 69, 1-29.

Fitzpatrick, R.W., Raven, M., Self, P.G., McClure, S., Merry, R.H. & Skwarnecki, M.S. (2000) Sideronatrite in acid sulphate soils in the Mt Lofty Ranges: first occurrence, genesis and environmental significance. In: J.A. Adams & A.K. Metherell (eds) – Soil 2000: new horizons for a new century, Australian and New Zealand 2nd Joint Soils Conference, Volume 2, 109-110.

George, R.J. (1967) Metamorphism of the Nairne pyrite deposit. Ph.D. thesis (unpubl.), University of Adelaide.

Giblin, A.M., A.R. Carr, A.S. Andrew and D.J. Whitford (1994) Exploration of concealed mineralization: Multi-isotopic studies of groundwaters. AMIRA Project 388. Regional hydrogeochemistry of the Kanmantoo fold belt. CSIRO Exploration and Mining Report 14R. 22 pp.

Skwarnecki, M.S., Fitzpatrick, R.W. & Davies, P.J. (2002a) Geochemical dispersion at the Mount Torrens lead-zinc prospect, South Australia, with particular emphasis on acid sulfate soils. CRC LEME Report 174, 68pp, 3 vols.

Skwarnecki, M.S., Fitzpatrick, R.W. & Raven, M. (2002b) Secondary lead minerals in acid sulfate soils, Mount Torrens prospect: implications for mineral exploration. In: V.P. Preiss (ed.) – Geoscience 2002: Expanding horizons. Abstracts, 16th Australian Geological Convention, Adelaide, 1-5 July 2002, No. 67, p.340.

Spry, P.G. (1976) Base metal mineralization in the Kanmantoo Group, South Australia: the South Hill, Bremer and Wheal Ellen areas. B.Sc. (Hons) thesis (unpubl.), University of Adelaide.

Toteff, S. (1999) Cambrian sediment-hosted exhalative base metal mineralization, Kanmantoo Trough, South Australia. Geological Survey of South Australia, Report of Investigations 57.

Wade, M.L. & Cochrane, G.W. (1952) Wheal Ellen mine. Mining Review, Dept Mines South Aust., 97, p.60-81.